QUILL
Quarterly Reports

February 2022 – April 2022

Contents

QUILL Quarterly Report

February 2022 – April 2022

Name:	Haris Amir		
Supervisor(s):	Prof John Holbrey		
Position:	Postgraduate PhD		
Start date:	10/01/2020	Anticipated end date:	09/30/2024
Funding body:	ESPRC/UKRI		

Design of New, Non-coordinating, and Hydrophobic Anions for Functional Ionic Liquids

New boron containing anions are of interest for the development of new ionic liquid anions with a wide range of potential applications including electro- and photo- chemistry, and for the separation and extraction of metals and waste. In this work, functional borate anions formed as complexes with O/N-chelators for ionic liquid applications have been designed and investigated.

A more efficient synthesis of different alkali salt borate anions incorporating O- and N/O-donor ligands is described. Thermogravimetric analysis (TGA) of the tetrabutylphosphonium salts was carried out to determine their thermal stabilities. Anion exchange is performed with trihexyltetradecylphosphonium chloride $[P_{66614}]$Cl to obtain ionic liquids with $[P_{66614}]^+$ cations combined with the different borate anions. The chloride content of, the trihexyltetradecylphosphonium salts will be determined using XRF, the aim will be to keep the chloride content below 250 ppm. The density and viscosity of the salts will be measured at various temperatures. The boron anions of interest are shown in Figure 1.
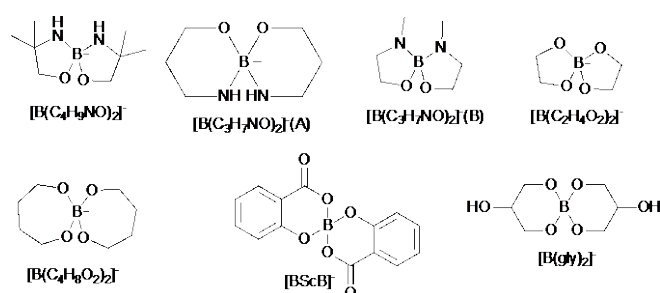
Figure 1 - Borate anions of interest

Crystallography of $[P_{4444}][B(C_3H_7NO)_2]$ based ionic liquids
Crystals suitable for single crystal X-ray diffraction were grown *via* the following methods, slow evaporation, slow cooling, vapor diffusion. in some cases, slow evaporation of dichloromethane from a concentrated solution of the salt gave bulky crystals, which made it difficult to perform single crystal X-ray diffraction. Vapor diffusion had the highest success of growing single crystals, the solvent chosen was methanol and the anti-solvent was diethyl ether. The X-ray diffraction data has given insight on into the structure of these salts, how they pack in a unit cell and intermolecular interactions between the cation and anions. Figure

2 shows the unit cell of $[P_{4444}][B(C_3H_7NO)_2]$ (A) alternate layers of the cation and anion are staked on top of each other. Similar conformation and packing are observed in the unit cells of each system. This packing was predicted when it comes to the unit cell of these compounds. The layers are likely held together with hydrogen bonding. Figure 3 confirms presence of hydrogen bonding for $[P_{4444}][B(C_3H_7NO)_2]$. The hydrogen bond between the nitrogen on the anion and a hydrogen on the alkyl chain from the cation. The oxygen on the anion also exhibited hydrogen bonding.
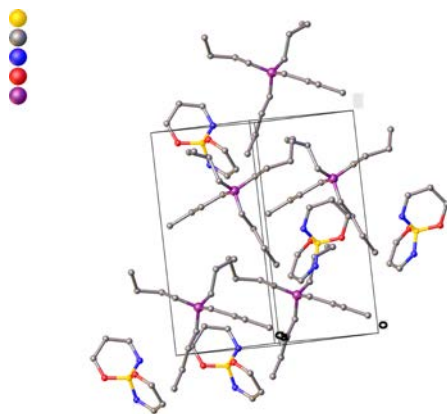
Figure 2 - Unit cell of $[P_{4444}][B(C_3H_7NO)_2]$
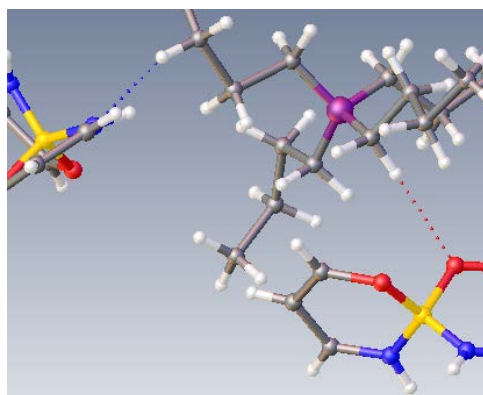
Figure 3 - Hydrogen bonding between $[P_{4444}]$ and $[B(C_3H_7NO)_2]$

TGA of $[P_{4444}]^+$ based ionic liquids

Table 1 - The onset and endset temperature of $[P_{4444}]$ based ILs

Ionic liquid	Onset temperature (˚C)	Endset temperature (˚C)
$[P_{4444}][BScB]$	302.2	352.7
$[P_{4444}][B(gly)_2]$	327.4	382.8
$[P_{4444}][B(C_2H_4O_2)_2]$	380.4	387.4
$[P_{4444}][B(C_4H_8O_2)_2]$	299.7	385.4
$[P_{4444}][B(C_3H_7NO)_2](A)$	345.8	389.8
$[P_{4444}][B(C_4H_9NO)_2]$	344.2	388.5
$[P_{4444}][B(C_3H_7NO)_2](B)$	486.7	589.5

As expected, the results showed, the bulky anions had a lower onset temperature. This is the temperature at which the compound first starts to decompose. The two which had the highest onset temperatures were the $[P_{4444}][B(C_2H_4O_2)_2]$ and $[P_{4444}][B(C_3H_7NO)_2]$. This could be due to the smaller and less bulky anion, as the anions are a boron centred 5 membered ring. However, it is interesting to note that $[P_{4444}][B(C_4H_9NO)_2]$ is also a boron cantered 5 membered ring but, have a similar onset temperature to that of the boron cantered 6 membered ring $[P_{4444}][B(C_3H_7NO)_2]$. This could likely be due to the two additional methyl groups on the carbon adjacent to the nitrogen. This will likely affect the intermolecular interactions between the cation and anion and prevent the ions to form strong hydrogen bond.

$[P_{66614}]^+$ based ionic liquids

$[P_{66614}]$ ILs were synthesised in the same manner as the $[P_{4444}]$ salts *via* anion exchange. The chloride content of each IL was measured using XRF analysis. This was done to unsure there was complete anion exchange between the borate anions and the chloride anion. This was so when the density and viscosity of the IL is measured the chloride anions does not affect the results. The chloride content for each IL synthesised was aimed to be ≤ 250 ppm, as below this the effect the chloride ions have are trivial. The density and viscosity of each IL will be measured at the following temperatures: 25˚C, 30˚C, 40˚C, 50˚C, 60˚C. IR analysis of the alkali salt, $[P_{4444}]$ salt and $[P_{66614}]$ IL to determine if the nitrogen and oxygen are bonded to the boron and not in an equilibrium, as shown below (figure 4) an example of the equilibrium between the desired 4 coordinate and the stable 3 coordinate for $[B(gly)2]^-$ boron species. IR should be able to detect if there are any OH or NH present for the respective anion or they are all bonded to the boron.
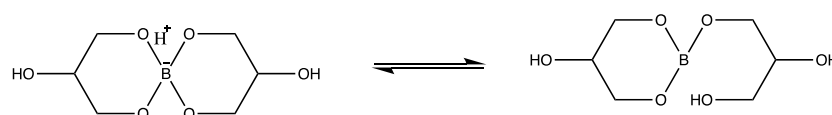
Figure 4 - Example of the equilibrium between the 4 and 3 coordinate boron

QUILL Quarterly Report

February 2022 – April 2022

Name:	Dominic Burns		
Supervisor(s):	Prof John Holbrey, Prof Gosia Swadzba-Kwasny and Dr Hye-Kyung Timken		
Position:	PhD Student		
Start date:	1st October 2019	Anticipated end date:	30st September 2023
Funding body:	EPSRC		

Recycle and Reuse of Process Water Through Sulfate Removal: Developing an Ionic Liquid Technology for Selective Anion Recognition and Extraction

Background

This is an EPSRC industrial CASE project in collaboration with Chevron, to explore technologies for the treatment of saline process water with the initial objective of selective sulfate removal from highly competitive aqueous streams. Extraction of hydrophilic oxyanions from aqueous solutions is an important industrial challenge across many sectors, from acid mine drainage to nuclear waste remediation, nuclear medicine, and general water treatment to address compliance with total discharge limits. Previously examined was the applicability of hydrophobic ionic liquid media for liquid-liquid extraction of a range of oxyanions from non-competitive aqueous solutions. It has previously been demonstrated that sulfate anions ($[SO_4]^{2-}$), can be extracted from 27.1 mM aqueous solutions with 57% efficiency using $[P_{66614}]Cl$, also known as CYPHOS® IL 101. A 2:1 chloride:sulfate anion exchange mechanism is found to overcome the Hofmeister series; however, this is strongly inhibited by excess chloride concentrations, for example from brine solutions.

Objective of this work

The main goal of this work is the selective removal of sulfate from sea water with a lesser emphasis on removal of sulfate from other competitive aqueous streams. A secondary goal of the research is to develop methods for the removal of toxic or valuable oxyanions of interest from water streams such as naphthenic acids, phosphates ($[H_xPO_4]^{y-}$), nitrate ($[NO_3]^-$), bromate ($[BrO_3]^-$), arsenates ($[H_xAsO_4]^{y-}$), pertechnetate ($[TcO_4]^-$), chromate ($[CrO_4]^-$) and selenate ($[SeO_4]^{2-}$).

Progress to date

Recently there have been two important results to outline; firstly Aliquat® 336, $[N_{1888}]Cl$, can extract a much greater amount of sulfate, 89.1%, than CYPHOS® 101 from the same conditions. It is unsure if this increased performance is due to the short methyl group allowing strong electrostatic attraction or due to the differences between the ammonium and phosphonium centres. A small series of hydrophobic ionic liquid chlorides have therefore been targeted for testing as outlined below. Secondly, 32.8% of sulfate can be extracted from a model sea water solution (2,600 ppm sulfate, 19,000 ppm chloride) if the solution is first

acidified with HCl to a pH < 1 and then extracted with Aliquat® 336. This may therefore be an effective strategy for sulfate removal from acid streams such as acid mine drainage etc.
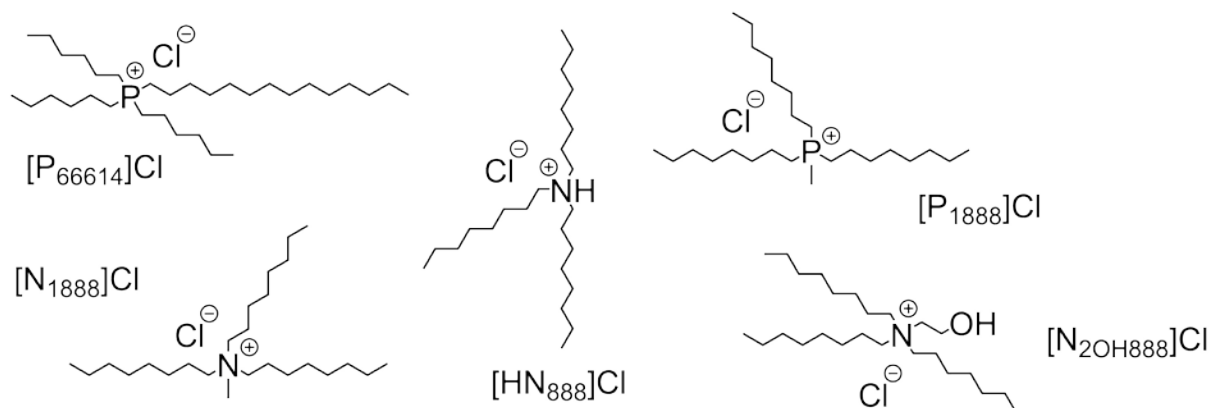
Figure 1 - Series of hydrophobic ionic liquids to be synthesised, characterised and tested
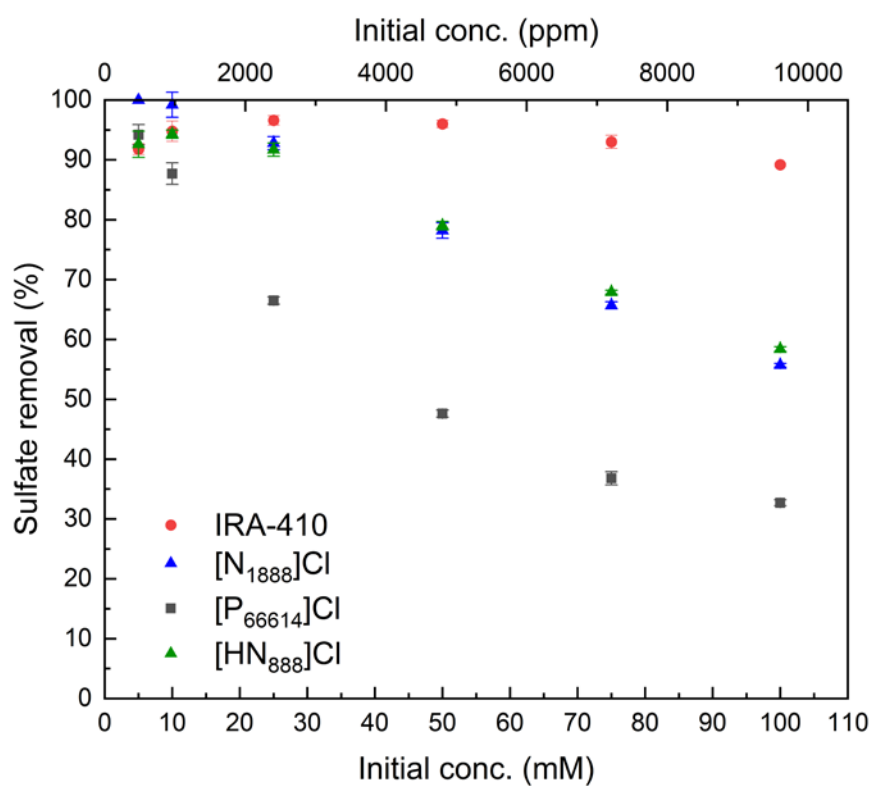
Figure 2 - Sulfate removal by each hydrophobic ionic liquid as a function of initial sulfate concentration with a solid ion-exchange resin (IRA-410) comparison
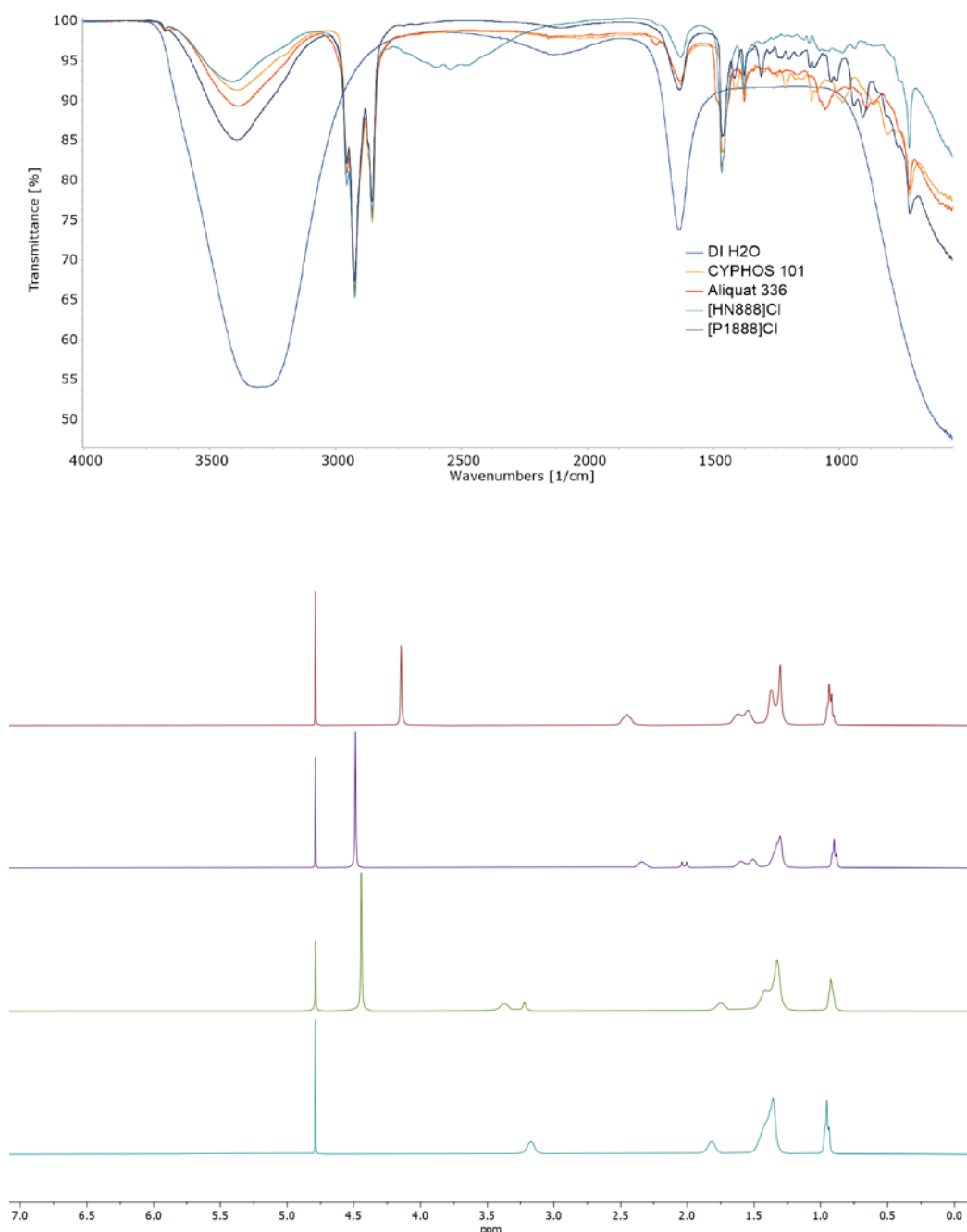
Figure 3 - (Top) FT-IR spectra and (bottom) neat ^{1}H NMR with D_2O capillaries of each water saturated hydrophobic ionic liquid phase showing how the environment of the saturated water changes depending on the structure of the cation

To date four of the five ionic liquids have been synthesised with the synthesis of [N$_{2OH888}$]Cl currently being investigated to completed this data set. Also currently being researched is the re-usability of Aliqaut 336 and extraction of other environmentally significant oxyanions.

Conclusions and future work

To conclude, a Series of hydrophobic ionic liquids have been synthesised with one more still to be completed. Each ionic liquid has been characterised in terms of density, viscosity, mutual solubility with water, NMR, FT-IR and sulfate extraction ability. Once this has been concluded then focus will shift towards anion receptors for a synergised ion-exchange extraction strategy.

QUILL Quarterly Report

February 2022 – April 2022

Name:	Andrew Forde		
Supervisor(s):	Dr Stephen Glover, Dr Rob Watson and Prof Peter Nockemann		
Position:	PhD Student		
Start date:	03/06/2019	Anticipated end date:	03/12/22
Funding body:	Horiba-MIRA & EPSRC		

Battery Thermal Management and Algorithmic 3D Temperature Prediction

A physics-informed neural network (PINN) for electrical battery predictions has been developed. This allows use of machine learning as an efficient method for voltage and SOC prediction while bringing added benefits over use of a standard neural network. PINNs require less data to train, are more interpretable, and generally perform better with unseen data as they are trained to obey governing equations

This work is being presented in a poster session at the Advanced Automotive Batteries Conference 2022, which compares the performance of the developed PINN against an equivalent standard neural network when given a very limited training dataset.

These results show the predicted voltage and SOC when the networks were given 60 seconds of various pulse discharge cycles, along with one charge cycle. As shown, the PINN outperforms the standard network in the training region (t<60) with smoother responses to changing current. However, in the unseen region, this gap in performance is exaggerated further, especially for SOC predictions
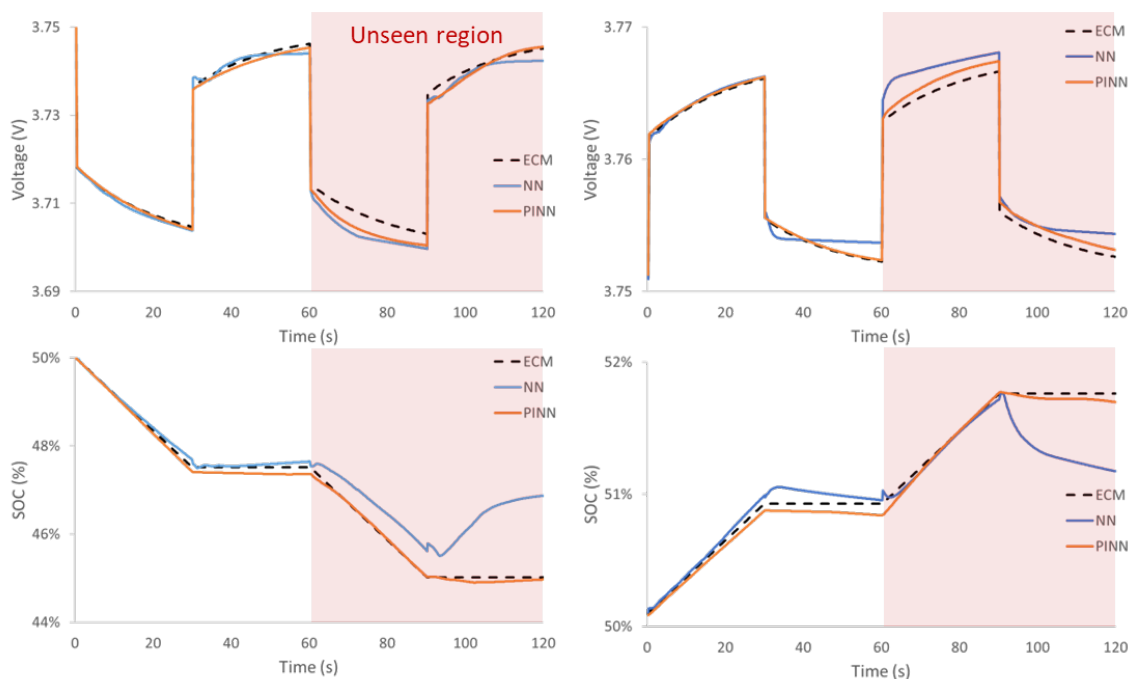
QUILL Quarterly Report

February 2022 – April 2022

Name:	Oisin Hamill		
Supervisor(s):	Dr Nancy Artioli and Dr Alex Goguet		
Position:	PhD		
Start date:	01/10/2019	Anticipated end date:	30/03/2023
Funding body:			

Mechanism Understanding of NOx Storage, Release and Reduction on Pt/Doped Ceria Catalysts

Background

Due to strengthening emission legislations in Europe, North America and the rest of the world, there is a need for further optimisation of existing emission after-treatment catalytic converters for automotive applications. New legislations focus primarily of NO_X abatement and consequently the exhaust emissions of lean-burn gasoline and diesel vehicles. After treatments systems must utilise new technologies to reduce this that offer low temperature activation and high stability.

High surface area ceria is successfully employed as an excellent support of metals (Pd, Rh, Pt, etc.) in commercial catalytic systems for the oxidations of carbon monoxide and propane and automotive emission control. Ceria is a unique material with a rich and complex chemistry. It possesses high oxygen storage capacity (OSC), a unique redox property by the cycle of Ce^{4+}/Ce^{3+} redox pairs and it can be further enhanced through using dopants. Platinum supported on ceria can show enhanced NO_X storage at low temperature, as reported in the literature, together with an improved carbon monoxide/hydrocarbon light off.

Ceria supported catalysts, in general, do not operate efficiently at low temperatures and therefore must be modified in order to overcome this problem. For this reason, addition of enhancing materials is currently being considered in detail. This addition of a material that increases the performance of an already functional catalyst is called doping. The main function of this dopant is to allow the catalyst to function outside of the normal working temperature range and operating conditions to increase catalyst efficiency.

It has been proposed that the dopants, such as rare-earth and transition metal oxides, increase the concentration of surface vacancies which affect the ionic conductivity, oxygen mobility and oxygen storage capacity of the ceria. It can be speculated that all these properties are responsible for the enhanced oxidation activity by promoting oxygen diffusion and formation of more "reactive oxygen" species. Furthermore, the oxygen species play a role in the mechanism of the reaction, favouring the NO_X storage.

Additionally, presence of dopants can reportedly modify the platinum reducibility and platinum-ceria interaction, allowing more readily activation during rich purge.

This project aims to better understand the NO_X storage mechanism on the doped materials and give new insights into the activation/lean deactivation mechanisms in the presence of different dopants.

Objective of this work

The main objective considered in this project is to improve the understanding of the NO_X storage mechanism, together with the mechanism of rich purge on ceria supported platinum. We aim to gain a deeper knowledge of the rich activation and lean deactivation mechanisms as well as determine the structure of the active sites under reaction conditions. We look to develop a method to differentiate between active species and spectator species through transient methods. We will also strive to develop a global kinetic model for the reaction and all involved species. This will enable the determination of the relative importance of different reactions within the catalyst bed as well as a measurement of the exact gas compositional conditions present during the reactions. With this approach in depth information relevant to mechanistic understanding and reaction engineering application will be obtained.

Progress to date
- XPS completed on ceria and alumina supported samples.
- EELS completed on 1Pt-Ce doped and undoped.
- Simplified catalyst testing to determine CO vs C3H6 oxidation.

Conclusions and future work
- Dispersion measurements.
- EXFAS characterisations.
- NSC test focusing on selectivity during reduction.

QUILL Quarterly Report

February 2022 – April 2022

Name:	Aloisia Elaine King		
Supervisor(s):	Prof John Holbrey and Prof Małgorzata Swadźba-Kwaśny		
Position:	PhD Student		
Start date:	01 Oct 2021	Anticipated end date:	March 2024
Funding body:	EPSRC		

Intrinsic FLP Systems in Ionic Liquids

Background

Frustrated Lewis acid/base pairs (FLPs) are potential metal-free alternatives to platinum group metal catalysts and have been shown to activate hydrogen for hydrogenation chemistry [1]. Typical examples of FLPs that have been studied are combinations of a sterically hindered bulky phosphine Lewis base paired with a strongly electrophilic Lewis acidic susbstituted borane.. While many of the advances in FLP chemistry have sought to exploit these bulky phosphine/borane pairs, less attention has been given to alternative acid/base pairs although examples with non-boron Lewis acid FLP components are known including N-alkylacridinium cations which have been show to exhibit FLPs chemistry when paired with lutidine (2,6-dimethylpyridine) as a base [2].

Objective of this work

The goal of this research is to develop organic FLPs (eliminating the need for Group 13-based Lewis acids) within an intrinsic IL medium in which, ideally, the potential catalyst concentration in the liquid is maximised and enables reaction intensification creating greener, sustainable chemistry through facile synthesis and replacement of both conventional solvents and platinum group metal catalysts.

Progress to date

In the previous report I explained in detail the premise behind the project: that the combination of an N-alkylacridinium cation (Lewis acid) with lutidine (Lewis base) previously reported as a dilute FLP system in organic media by Clark and Ingleson [2] could, potentially be developed into an intrincially ionic liquid system in which hydrogen activation and splitting by the Lewis acid/base pair would lead to formation of neutral hydro-acridine and protonated lutidinium cationic species maintaining the overall ionicity of an ionic liquid/base mixture. Three N-alkyl-acridinium salts and N-protonated heterocyclic ionic liquids had been successfully synthesised and characterised as precursors for FLP studies. The N-alkylacridinium bis{trifluoromethylsulfonyl}imide ([R-Ac][Tf$_2$N]) salts synthesised are highly soluble in H-lutidinium and H-picolinium bis{trifluoromethylsulfonyl}imide ([H-lut][Tf$_2$N] and [H-pic][Tf$_2$N]) ionic liquids which contrasts with the reported poor, and limiting solubility of N-methylacridinium salts in organic solvents. The H$_2$ screening experiments, initiated previously are under detailed investigation, addition of low pressure gaseous H$_2$ to [R-Ac][Tf$_2$N]/[H-lut][Tf$_2$N]/lutidine mixtures results in the generation of proton NMR signals

that can be assigned to formation of the hydro-acridine molecular adduct (addition of a hydride) and collapse of the lutidine signals into bulk IL H-lutidinium cations (protonation). The NMR measurements were challenging due to current low concentrations of FLP components in the protic IL solvent, and method development is required to overcome these challenges. Reactions were performed with 0.2 mmol of LA/LB components dissolved in 1.2 cm3 of IL to act as solvent, consistent with literature work in dichloromethane. However, samples taken from this FLP/IL/H2 mixture for screening after dilution in CD2Cl2 for subsequent 1H NMR analysis display a pronounced concentration dependent chemical shift across many of the proton signals making qualitative analysis impossible. So we are currently testing and devising a new system to overcome this challenge. Earlier proposed work to generate N-alkyl-dicyanopyridinium cations, as analogues of the [N-Ac]+ has not yet been started, due to the focus on establishing the feasibility of generating the H2-activating [R-Ac][Tf2N]/[pic/lut][Tf2N]/Lut FLP system and 1H NMR screening of this. Additionally, our LA FLP components (N-alkylated acridinium [Tf2N]) is fluorescent and if this fluorescence changes upon addition to a H2 rich environment there is potential for this system to also act as a fluorescent probe for H2.In summary, much progress has been made to test this novel Intrinsic IL Organic based FLP system to date and my abstract that I submitted for the EUCHEMSIL Conference was accepted. I also received RSC Funding of £ 500 for my attendance at this event.

Conclusions and future work

I will continue to make the materials that I need to carry out the H_2 screening experiments. Also I will continue doing these H_2 activation screening experiments and analysing the copious results in dept. Next month I will attend the EUCHEMSIL conference on IL's in Greece and give a poster presentation, outlining my results to date. To conclude, I hope to report on the summary of these H_2 activation experiments by the next report and also to have optimised the various alkylating reactions mentioned.

References

1. D. W. Stephan and G. Erker, *Angew. Chem. Int. Ed.,* 2010, 49, 46–76.
2. E. R. Clark and M. J. Ingleson, *Angew. Chem., Int. Ed*., 2014, 53, 11306–11309.

QUILL Quarterly Report

February 2022 – April 2022

Name:	Sanskrita Madhukailya		
Supervisor(s):	Prof John Holbrey and Dr Leila Moura		
Position:	PhD student		
Start date:	19th April 2021	Anticipated end date:	20th April 2024
Funding body:	Tezpur University/QUB joint PhD scholarship		

LCST Phase Behaviour of Substituted Tetrabutylphosphonium 5-Phenyltetrazolate/Aqueous Mixtures

Background

In the previous report, synthesis of tetrabutylphosphonium 5-(2-hydroxyphenyl)tetrazolate. [P$_{4444}$][2-OH-PhTet] and tetrabutylphosphonium 5-(4-methylphenyl)tetrazolate, [P$_{4444}$][4-Me-PhTet] was shown to be synthesized. The former was tested for the biphasic behaviour for few mass fraction compositions with normal water. However, detailed investigation along with comparisons with the already reported ionic liquids are performed in this section. Additionally, synthesis of some dicationic ionic liquids is also performed.

Objective of this work

The ultimate aim of this work is to understand and explain the lower critical solubility temperature (LCST) phase behaviour of some ionic liquids, to know the boundaries and frame a methodology for synthesising such ionic liquids that can behave as a potential draw solute to be used in the forward osmosis process for sea water desalination. In this process, a range of ionic liquids with the tetrazole moiety will be synthesised, tested, and compared with the existing ones, based on the type of anion or cation chosen, that can affect the phase behaviours.

Progress to date

1. The prepared tetrabutylphosphonium 5-(2-hydroxyphenyl)tetrazolate was tested for its biphasic behaviour for 10% to 80% mass and mole fractions using the instrument crystal 16. The phase diagram and the turbidity curve for 50 wt% of [P$_{4444}$][2-OH-PhTet]
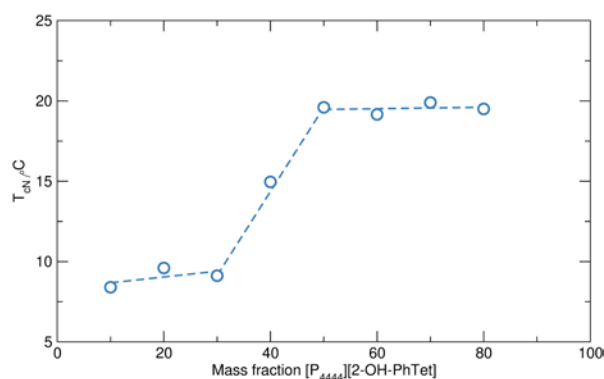
Figure 1 - Phase diagram for mass fraction composition of [P$_{4444}$][2-OH-PhTet] vs cloud point temperature
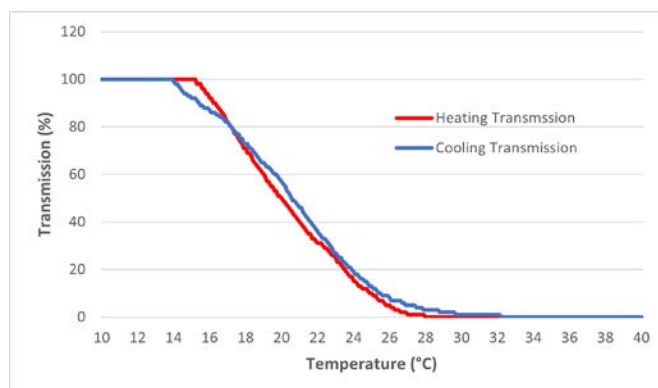
Figure 2 - Turbidity curve for 50 wt% [P4444][2-OH-PhTet]

2. Comparison of the biphasic behaviour with the already reported [P4444][PhTet] by Leila *et.al.*[1], and [P4444][Sal] by Ohno *et.al.*[2] is carried out.
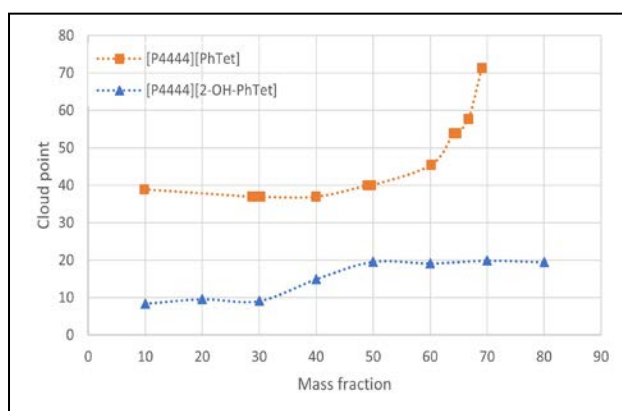
Figure 3 - Difference in the cloud point for the [P4444][PhTet] & [P4444][2-OH-PhTet]
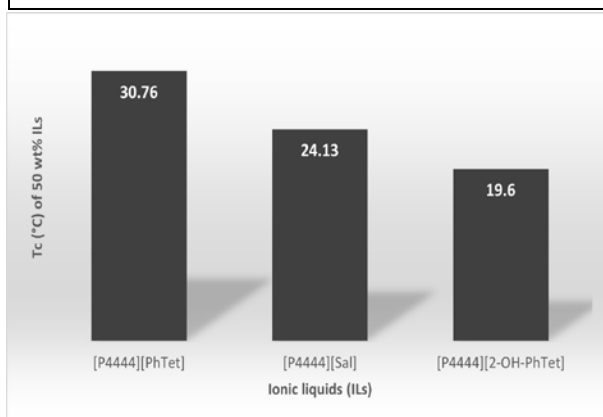
Figure 4 - Comparison of the cloud point temperature for 50 wt% of three ionic liquids with 3.5 wt% saline water (mimic sea water)

3. Synthesis of a dicationic ionic liquid, 1,5-pentanediyl-bis(tri-n-butylphosphonium)di(5-phenyltetrazolate) for testing its phase behaviour: 11.8 mmol of already prepared 1,5-pentanediyl-bis(tri-n-butyl phosphonium)dibromide was dissolved in sodium tetrazolate solution in water and was allowed to stir for 2 hours (until phase separation) at a temperature of 60 degrees.
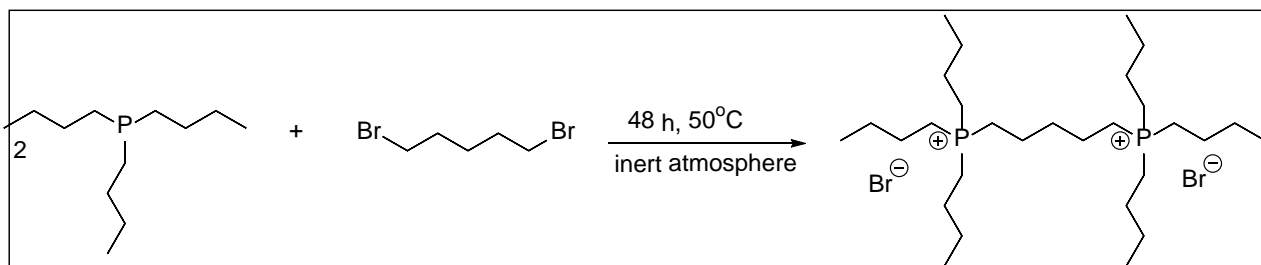
Figure 5 -: Synthesis of the 1,5-pentanediyl-bis(tri-n-butyl phosphonium)dibromide from tributylphosphine and 1,5-dibromopentane
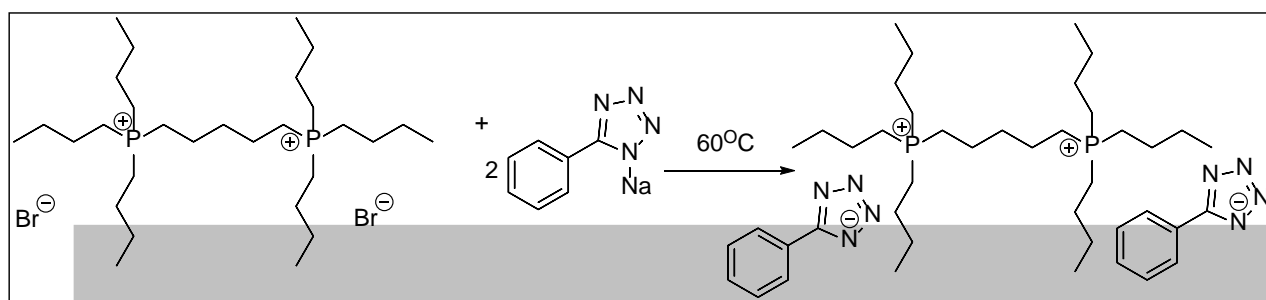
Figure 6 - Synthesis of the dicationic ionic liquid, 1,5-pentanediyl-bis(tri-n-butylphosphonium)di(5-phenyltetrazolate).

Conclusions

1. The phase diagram for the tetrabutylphosphonium 5-(2-hydroxyphenyl)tetrazolate shows that the cloud point somewhat remains constant at higher compositions.
2. On comparison with the [P_{4444}][PhTet] and [P_{4444}][Sal], it can be observed that the cloud point temperature decreased for the similar composition with the saline water mimicking the sea water.
3. The formation of the dicationic ionic liquid was confirmed using the ^{1}H and ^{31}P NMR as shown. The presence of the peak at 2.1-2.2 ppm indicates the presence of the proton adjacent to the quaternary phosphonium cation. This was further confirmed form the ^{31}P peak at 33.9 ppm.
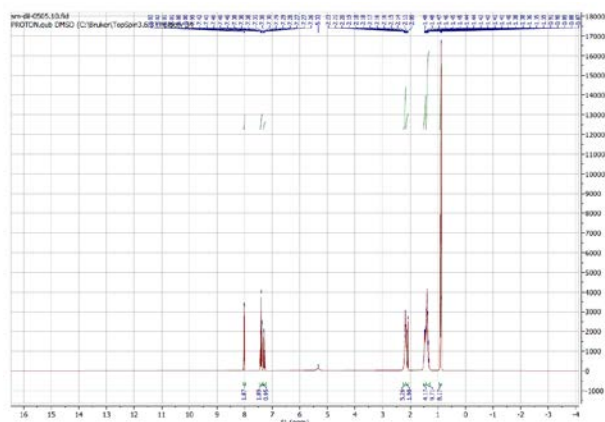
Figure 7 - ^{1}H NMR of 1,5-pentanediyl-bis(tri-n-butylphosphonium)di(5-phenyltetrazolate)
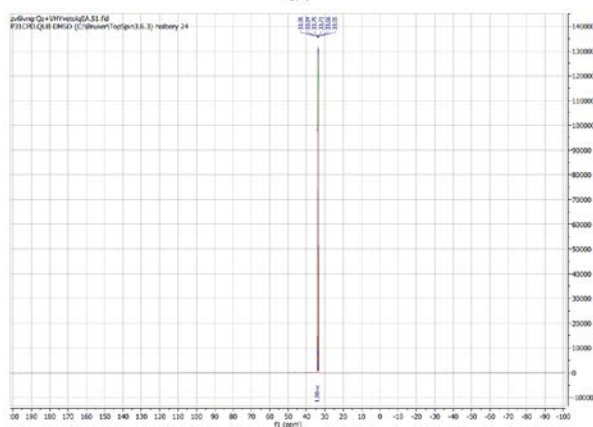
Figure 8 - ^{31}P NMR of 1,5-pentanediyl-bis(tri-n-butylphosphonium)di(5-phenyltetrazolate)

4. The synthesised dicationic ionic liquid however did not show any LCST phase behaviour. The solubilities/hydrophilicity index values are however yet to be investigated.
5. Further studies on dicationic ionic liquid with different alkyl linker chains and anions/cations, to understand their effects in the hydrophobicity/hydrophilicity of the prepared ionic liquids are to be performed.

Bibliography

1. Moura, L., Brown, L. C., Blesic, M. & Holbrey, J. D. LCST Phase Behavior and Complexation with Water of an Ionic Liquid Incorporating the 5-Phenyltetrazolate Anion. *ChemPhysChem* **18**, 3384–3389 (2017).
2. Ando, T., Kohno, Y., Nakamura, N. & Ohno, H. Introduction of hydrophilic groups onto the ortho-position of benzoate anions induced phase separation of the corresponding ionic liquids with water. *Chem. Commun.* **49**, 10248–10250 (2013).

QUILL Quarterly Report

February 2022 – April 2022

Name:	David McAreavey		
Supervisor(s):	Dr Stephen Glover, Dr Oana Istrate and Prof Peter Nockemann		
Position:	PhD student		
Start date:	1st October 2021	Anticipated end date:	31st March 2025
Funding body:	Department for the Economy		

Design and Development of an Effective and Interconnected Smart Fire Suppression System for Lithium-ion Batteries in Electric Vehicles

Background

As many countries around the world begin to implement their plans to ban the sale of new petrol and diesel vehicles in the coming decades, there is a clear shift occurring towards electrification of transportation. However, there are several challenges that should be addressed if mass adoption of these vehicles is to be successful. Chiefly among which are the needs to extend range and improve battery safety. Depending on the sources used it can be argued that EVs do have a good battery safety record and the number of electric vehicle fires that occur are relatively low. Tesla's 2020 vehicle safety report claims that one of their vehicles is almost ten times less likely to be involved in a vehicle fire than the average vehicle on the road in America per mile driven, based on data from the national Fire Protection Association and US department of transportation. Contrary to this, in London in 2019 based on data from the London Fire Brigade the incident rate when adjusted for the number of EVs and IC vehicles on the road is more than twice as high for EVs. Regardless of the exact frequency, due to the nature of these thermal events they can often initiate thermal runaway, meaning that it is extremely difficult to extinguish as well as having the potential to burn both hotter and longer than a typical IC vehicle fire. The primary concern is of course for the safety of the occupants of the vehicle and the potential danger to their health. Additionally, an EV has the potential to ignite in scenarios when nobody is around, usually an IC vehicle will ignite in use as this is when the highest temperatures are experienced. EVs on the other hand can ignite under circumstances such as when charging. This means that the thermal runaway process may go unnoticed for some time as well as likely being close to a home or garage causing significant property damage.

An additional concern surrounding the adoption of EVs is the level of media attention that EV fires receive. Despite being relatively infrequent especially due to the low total market share they hinder the adoption of these vehicles as well as causing the loss of resources that was originally carbon intensive to produce.

Objective of this work

The ultimate goal is to develop a fire suppression and thermal management system that can be realistically employed in a vehicle. This work may only achieve a step in this development,

for such a suppression system. It is vital to consider that such a system must be compatible with thermal management systems as the implementation of a fire suppression system without an appropriate thermal management system essentially renders the vehicle useless. This means that a vehicle has the ability to keep the cells within its pack in the optimal temperature range, promoting longevity. As well as having a sufficient suppression system that is able to prevent the propagation of thermal runaway between cells in the event of a fault or road traffic collision.

Progress to date

During this quarter the preliminary modelling began in earnest with two pieces of literature being replicated to confirm the function of the MATLAB models developed. The first of these was an experiment that used phase change materials in a multi cell array as a means of thermal management. A range of simplifying assumptions were made to reduce the computational expense of running these models, as well as reduce complexity.
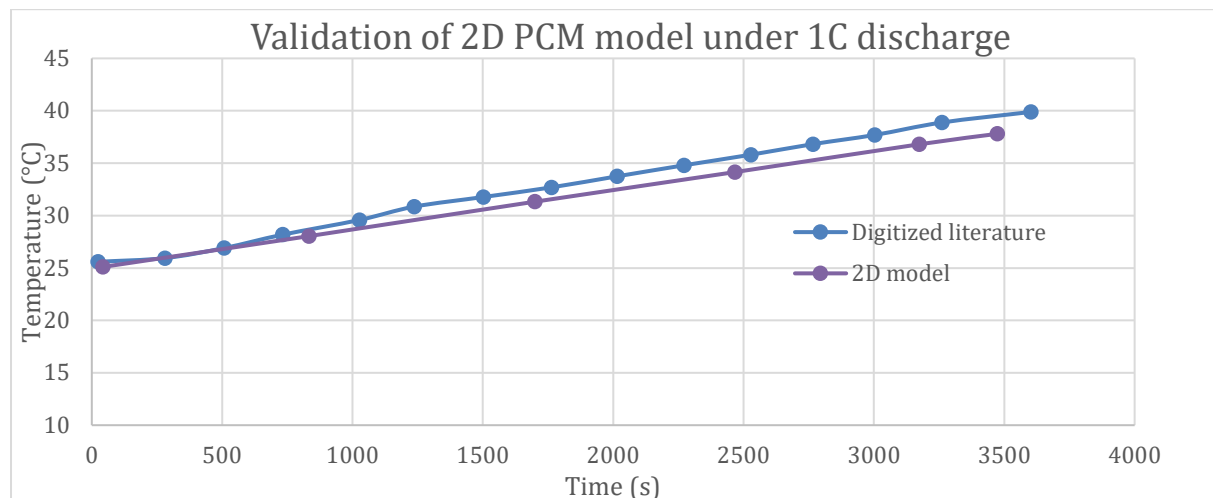
In this report a grid of twenty cells with PCM between them underwent a range of tests including thermal management under a 1C discharge. The rate of heat generation was included and was approximated as a linear profile. The data was generated by digitizing the graphs provided and a trendline was then fitted. The linear trendline had an R squared value of 0.997 proving to be adequate for the fundamental validation of this 2D model. This model validated the underlying mechanics used but the assumptions made have had some effect on accuracy.

Following this a second model was developed to replicate the results of a liquid cooling set-up, this would validate the underlying convection heat transfer mechanics in the model that could be taken forward to the more advanced model. The simulation set-up to be replicated included a number of 18650 cells being cooled indirectly by water channels through aluminium blocks of varying contact area.

In a similar vein to the first paper a smaller domain of the full simulation was taken using lines of symmetry in the geometry to simplify the problem, as before a range of other assumptions were used to simplify the problem. The results obtained are in reasonable agreement with those presented in the literature but not as close as would have been expected.

Convection model validation

Y-axis: Cell Surface temperature (°C)
X-axis: Time (s)

Legend:
Cell 6 Literature
Cell 5 Literature
Cell 4 Literature
Cell 3 Literature
Cell 2 Literature
Cell 1 Literature
Cell 6 MATLAB
Cell 5 MATLAB
Cell 4 MATLAB
Cell 3 MATLAB
Cell 2 MATLAB
Cell 1 MATLAB
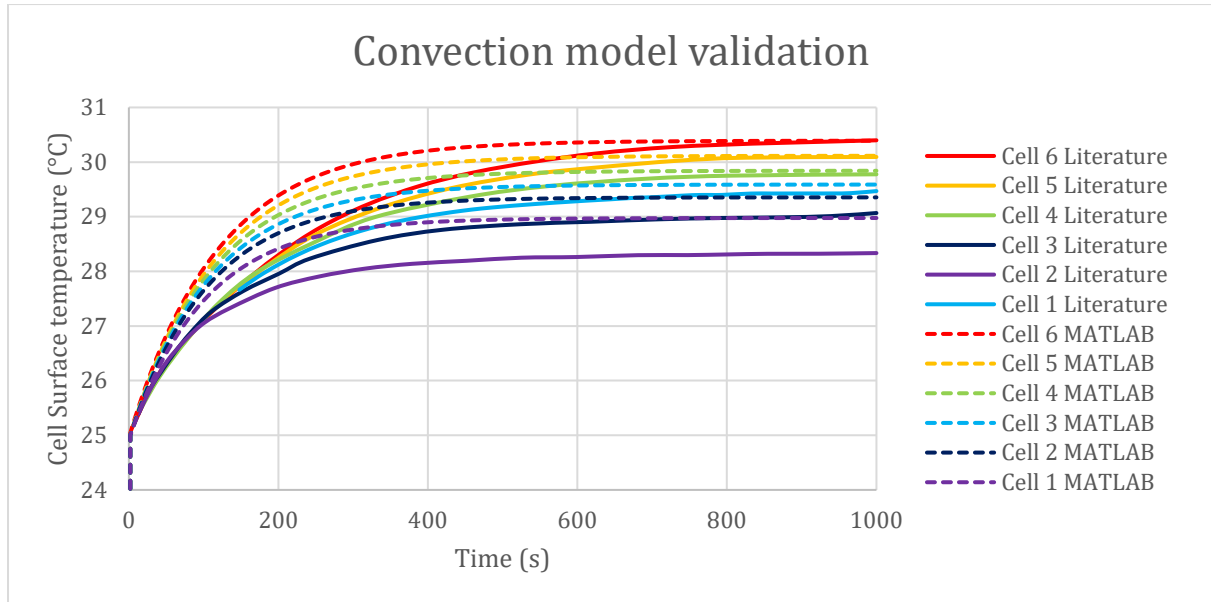
The next step in this process was to develop a combined thermal management and thermal runaway prevention model based on a hybrid cooling set up to assess the feasibility of the parameters mentioned previously. To do this a number of simplifications were again applied. The intention was to heavily base this modelling on commercial designs. As one of the market leaders the Tesla style system was chosen to be the main guiding design. They also use the cylindrical cells which lend themselves to implementation of PCMs as they have space between the cells, that can be used with reduced effect on packing efficiency. However, it was decided to model the slightly older cell format of 18650 cells which tesla are now moving away from, however there is a significantly reduced amount of information on the newer cells making it much more difficult to model them. In these older pack setups there was a single liquid cooling ribbon that was responsible for cooling one full module of 444 18650 cells. In an ideal scenario this full module would be modelled as the temperature of the liquid coolant will be continually rising throughout the module affecting the thermal gradient cooling the cells. However due to the significant damage that non uniform temperature can have on a pack it is expected that under normal operation the difference shouldn't be too significant, and by only modelling a portion of the pack the size of the simulation can be significantly reduced.

This model used significant portions of code from the previous models with a couple of additions. These included a trigger cell profile, this was a mechanism of setting the temperature profile to emulate those of other experiments conducted in literature. This was once again a simplification as ideally heat generation profiles would have been used as the use of a temperature profile wasn't able to interact with the cooling set up. This means that at a given time the temperature will be the same regardless of the cooling setup.

A range of simulations were run using one of the most energetic temperature profiles detailed in literature of an 18650, which also had the highest peak temperature from experimental study of the cooling effect based on a thermal abuse setup. A profile from a cell that has undergone nail penetration would have had a significantly lower peak temperature but it was deemed important to consider the worst case scenario for a cell under thermal decomposition. A number of cell spacings and cooling channel placements were considered. The early fundamental calculations conducted suggested that a weight increase in the order

of 50% may be expected as a worst case which equates to a cell spacing of around 12mm. The results from the combined model suggested that with a pure PCM, in this case paraffin, as one of the most widely used the neighbouring cells to the trigger cell spacing was able to be set at 5mm. With the cells in direct contact with the liquid cooling channels the neighbouring cell temperature peaked at 88.06 degrees which is between the trigger points set depending on the cell SOC.
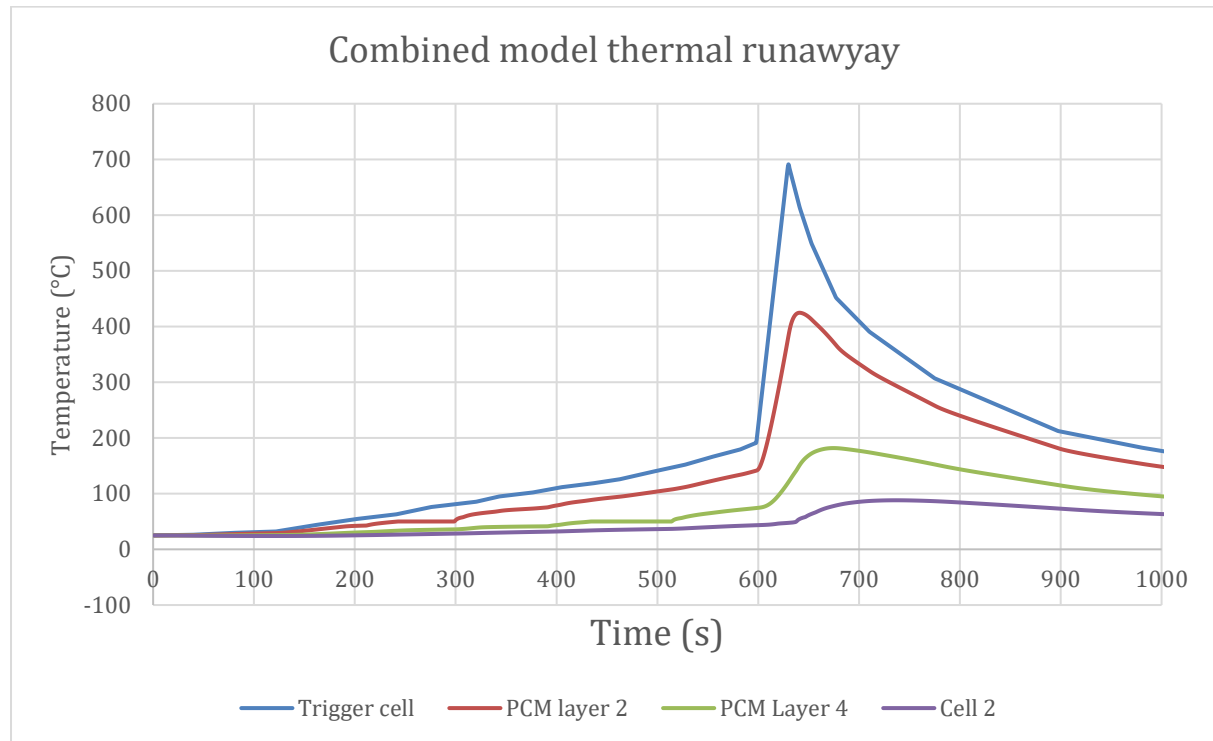
When the same simulation was run with a hybrid PCM with a thermal conductivity of 1.1W/mK and as a consequence a reduced latent heat the maximum temperature of the second cell spiked to 195.5 degrees. Even when the power of the liquid cooling was artificially increased by 50% to observe the sensitivity the peak temperature of cell 2 only dropped to 181.656 degrees, suggesting the cooling system capacity would need to be increased significantly if a composite PCM was to be used.

The benefit of using a composite PCM is of improved thermal management of the system during its operational life. With a 5mm spacing and phase change material of conductivity 0.2 w/m/k under a 2C discharge the cells ended with a temperature delta of the cell of 5.35 degrees between the cell centre and exterior after 1200 seconds. With an increase of the thermal conductivity to 1.1 W/mK a decrease in this temperature delta to 3.12 degrees was observed. This supports the statements made by Zhang that reduced thermal conductivity to enhance thermal runaway protection will be opposed to the goals of effective thermal management.(57)

Weight and volume increase
The main penalties of including a thermal runway prevention system in a vehicle is the weight and volume increase. In Tesla's 2021 battery day event they proposed a number of innovations that they plan to implement in the coming years. One of these was the use of

structural battery packs that will lead to a 10% weight reduction in the body of the vehicle which opens the door to a "14% range increase opportunity", by contrast the inclusion of 5mm spacing with pure paraffin between the cells results in a 19.6% weight increase of an 85kWh Tesla model S. If the assumption is made that this relationship is relatively linear then this suggest that the inclusion of this system could result in an approximate 30% decrease in range. As mentioned previously the main concern of most consumers is range, although that demand appears to be declining a system that improves safety at a significant determent to range would be unlikely to gain mass adoption. Furthermore, the increase in pack size would also be close to 20% in length and width which may struggle to fit within the chassis of current vehicles.

Conclusions and future work

The promise shown in the literature has not been mirrored by the results from the simulation and the question has to be asked why there is this disparity. Some literature tests were carried out in open air so a significant amount of heat would be lost to the air through convection. In the model temperature profiles were used which were not affected by the cooling due to the complexity of the temperature dependent heating rate. The nail penetration tests also seemed to be more sedate than the thermal abuse tests.

Due to the weight and volume penalties that were originally raised as a potential issue being confirmed, it has been highlighted that a targeted form of suppression is going to be the only version of a thermal runaway prevention system that is going to satisfy the weight requirement of this application.

Therefore, the most suitable direction for the project is to consider liquid gas PCMs with the intention of implementing a targeted suppression system. Using liquid gas phase change materials will undoubtedly increase the complexity of the system but hold the potential to reject far larger amounts of heat energy in a more compact system without compromising vehicle range.

Name:	Sam McCalmont		
Supervisor(s):	Dr Leila Moura, Prof John Holbrey and Prof Margarida Costa Gomes		
Position:	PhD		
Start date:	Jan 2020	Anticipated end date:	2023
Funding body:	EPSRC Doctoral Training Partnership		

Chemisorbent Materials for Olefin and Paraffin Separation

Background

Separation of light olefins from their paraffin counterparts have been described as one of the seven chemical separations to change the world.[1] Global annual production of light olefins exceeds 200 million tons, about 30 kg for each person on the planet. The current method for their separation is cryogenic distillation, one of the most energy-intensive processes in the industry. Alternative methods can focus on the olefin being selectively captured either through a physical interaction (physisorption) or chemical reaction (chemisorption).

One class of alternative sorbents are ionic liquids (ILs). However, so far, IL physisorbents have not demonstrated sufficient efficiency in either selectivity or capacity to compete with current technologies.[2] Complexation of ethylene through its double bond with silver and copper ions has been used for chemical separation of olefins and paraffins. However, other components of raw gas feeds, such as acetylene, can react with the silver and become explosive. This has prevented the uptake of these materials into large scale processes.

Objective of this work

To develop and test new chemisorbent materials for the separation of light olefins and paraffins; to achieve high capacity combined with selectivity for the selected materials. To investigate, and rationalise, selectivity and capacities of chemisorbents based on measurement of gas solubility and partitioning from model industrial gas stream compositions and conditions.

Progress to date

Over the last three months, investigation of two groups of ionic liquids has been undertaken. The two groups are: (i) cyanopyridinium based ionic liquids[3] and (ii) ionic liquids incorporating dissolved metal species (not silver or copper which have been previously studied by other research groups).Both groups of ionic liquid systems are being examined for ethylene/ethane separation via the gas solubility system (GSS) and screening method.

Cyanopyridinium ionic liquids synthesised, and previously reported (butyl-4-cyanopyridinium bis(trifluoromethylsulfonyl)imide ([C$_4^4$CNPy][NTf$_2$]) and butyl-3-cyanopyridinium bis(trifluoromethylsulfonyl)imide ([C$_4^3$CNPy][NTf$_2$]) (figure 1) have moved out of the screening method and are focusing on completing the measurements on the upgraded GSS. This will involve pure ethylene and ethane tests, and mixture of ethylene/ethane test.
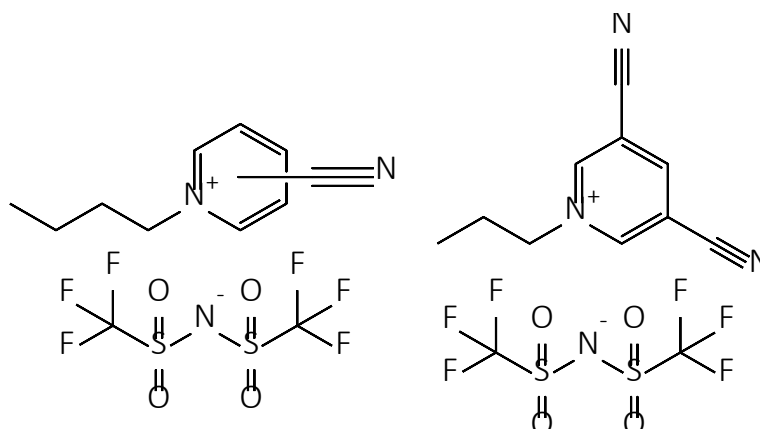
Figure 1 - 1-Butyl-*n*-cyanopyridinium bis(trifluoromethylsulfonyl)imide (*n* = 3 or 4, left) and butyl-3,5-cyanopyridinium bis(trifluoromethylsulfonyl)imide (right)

As was described in the previous report, ethylene and ethane solubilities were found to be similar in both [C$_4$^{4}CNPy][NTf$_2$] and [C$_4$^{3}CNPy][NTf$_2$], with ethylene solubility being marginally higher than that of ethane. When compared with the reference benchmark ionic liquid, [C$_4$mim][NTf$_2$], as shown in figure 2, [C$_4$mim][NTf$_2$] exhibits greater solubilities of ethylene than [C$_4$^{4}CNPy][NTf$_2$] and [C$_4$^{3}CNPy][NTf$_2$]. This is consistent with the general trend across ethylene/ethane solubility and separation screening in the literature that shows that ethylene has a reduced solubility in ionic liquids containing nitrile functional groups compared to [C$_4$mim][NTf$_2$].

One parameter that has been started to be investigated is the comparison of research scale screening strategies and methods with approaches conducted on an industrial scale, i.e. the pathway from low to higher TRL. In terms of a research scale, individual gas solubilities are studied for each sorbent. In the industrial scale up, both gases (among other gas impurities) are mixed, and this is the reasoning behind the separation. Following the single gas screening with [C$_4$^{4}CNPy][NTf$_2$], mixed ethylene/ethane gas systems are under investigation and initial results are shown in figure 3. The uptake of ethylene in the IL decreases from pure ethylene solubility to the solubility of ethylene from the mixed gas stream. This is expected as there is now competition between ethylene and ethane solubility, due to the reduced partial pressure of each individual gas component.
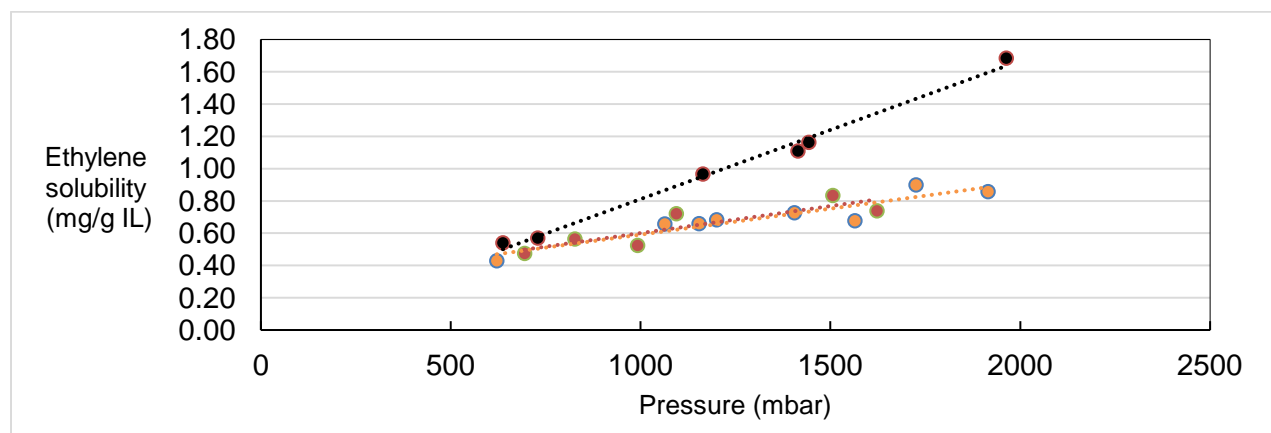
Figure 2 - : Initial uptakes of ethylene for [C$_4$^{4}CNPy][NTf$_2$] (●), [C$_4$^{3}CNPy][NTf$_2$] (●), and [Bmim][NTf$_2$] (●)
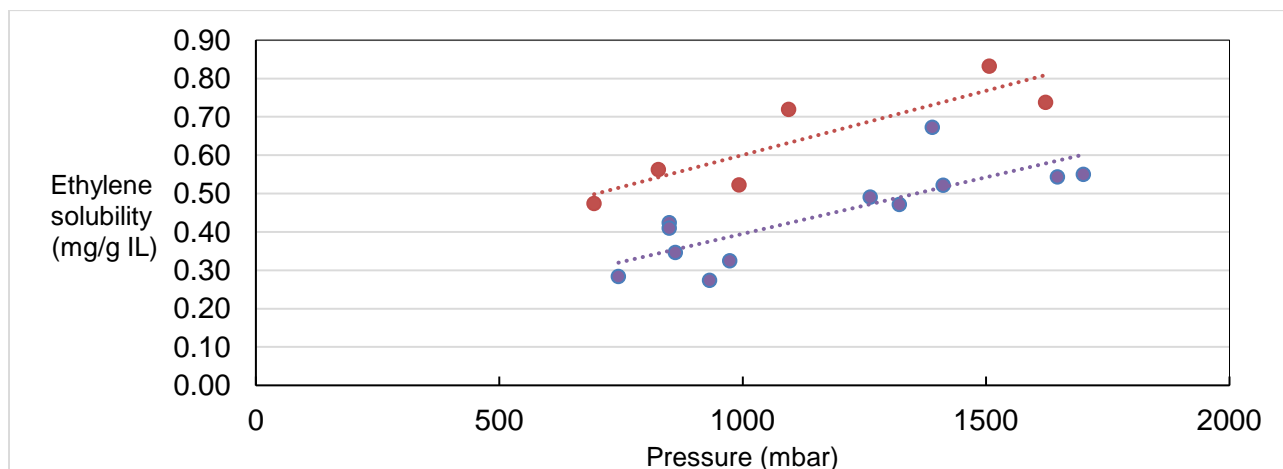
Figure 3 -Comparing the solubility of ethylene in $[C_4^4CNPy][NTf_2]$ from two different sources: pure ethylene (●) and from a mixture of ethylene and ethane (●).

The next stages include finalising the results with $[C_4^4CNPy][NTf_2]$ and $[C_4^3CNPy][NTf_2]$ in the GSS. New ionic liquids containing di-cyanopyridinium cations (shown in figure 1, right) are currently under synthesis and will be investigated to further explore and rationalise the potential interaction mechanisms in regard to ethylene and ethane solubility, allowing for more analysis on the impact on additional nitrile functional groups in the ionic liquid.

The second area of interest has been introducing different metal species in exchange for silver and copper. The basis for the separation is the formation of a reversible π-bond complexes between the metal ions and ethylene. This involves the back donation of electrons from the filled d-orbitals of the metal to the π*-orbitals of the ethylene. A number of different transition metal ions, solubilised in IL are being investigated, involving screening and assessment of a range of metals in these two base ionic liquids, with solubility tests (to determine metal salt solubility and miscibility in the ionic liquids) and then measurement of gas solubility of ethylene, ethane, and ethylene/ethane mixtures as a function of partial pressure.

The first group of experiments were based on dissolving different metal salts into $[C_4mim][NTf_2]$ and comparing the effect the metal has on ethylene solubility compared to that of pure $[C_4mim][NTf_2]$. A range of different metal salts were tried, and how soluble they were in $[C_4mim][NTf_2]$ was determined . Iron and Zinc salts proved soluble at 5% and 10% molar fraction for example. The screening method was utilised again to determine the solubility of ethylene and ethane. However, it was found that the ethylene solubility did not change with the presence of the dissolved metal salts, or with the concentration of the metal salts compared to that of pure $[C_4mim][NTf_2]$. A comparison was then completed utilising silver salts (established to form that bond with ethylene) to determine if the screening method could determine the change in solubility of ethylene and ethane. The ethylene uptake increased from the average trend. This is an ongoing study.

Halometallate ionic liquids have also be looked into as a possible group of ionic liquids for ethylene and ethane solubility.[4,5] The halometallate ionic liquid $[C_4mim][FeCl_4]$ has been used

in propylene/propane separation and was used as a base test for ethylene and ethane separation.[5] [C$_4$mim][FeCl$_4$] and [C$_4$mim][ZnCl$_4$] were produced and resulted in liquid form, where others transitional metals formed solids, such as manganese. The [C$_4$mim][FeCl$_4$] and [C$_4$mim][ZnCl$_4$] so far have been tested for ethylene solubility, and what was found was that [C$_4$mim][FeCl$_4$] has similar solubility of ethylene as that of [C$_4$mim][NTf$_2$], possibly resulting in the need not to work with lithium bis(trifluoromethylsulfonyl)imide and instead work with iron (III) chloride which is substantially cheaper, although hydrolysis is likely to be a barrier to practical development. Ethylene was found to have lower solubility in [C$_4$mim][ZnCl$_4$] compared to [C$_4$mim][NTf$_2$] and [C$_4$mim][FeCl$_4$].
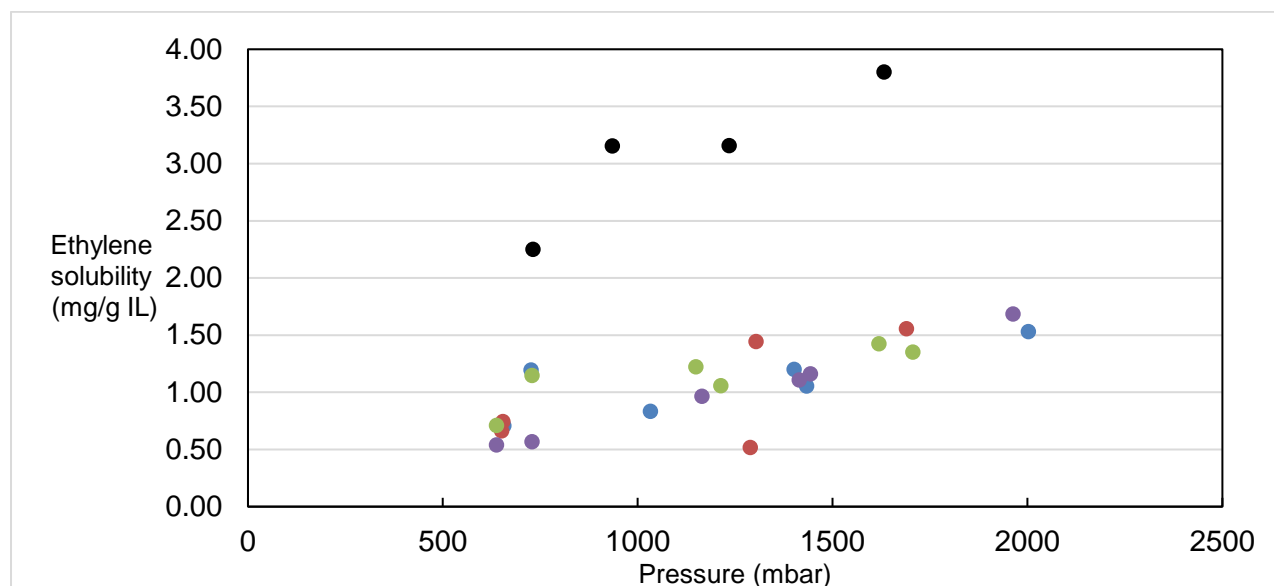
Figure 4 - The additional of different metal salts to [C$_4$mim][NTf$_2$]. Addition of 10% molar fraction ZnBr$_2$ (●), 5% molar fraction ZnBr$_2$ (●), 5% molar fraction FeCl$_3$ (●), 5% molar fraction Ag[NTf$_2$] (●) and pure [Bmim][NTf$_2$] (●) as reference
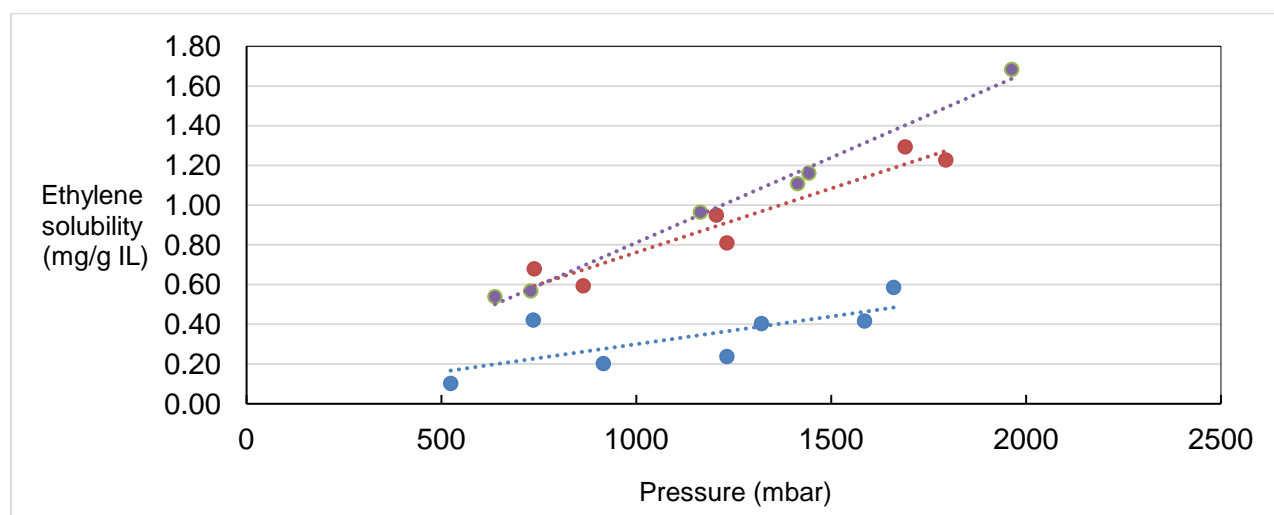
Figure 5 - Ethylene solubility in halometallate ionic liquids; [C$_4$mim][FeCl$_4$] (●), [C$_4$mim][ZnCl$_4$] (●), and [C$_4$mim][NTf$_2$] (●) as a function of ethylene pressure

Conclusions and future work

In the coming weeks, the plan is to move forward to test the materials created with a gas mixture to closer study the separation potential between ethylene and ethane, especially with the halometallate ionic liquids. Moving forward also with the di-cyanopyridinium ionic liquid as well.

References:

1.   D. S. Sholl and R. P. Lively, *Nature*, 2016, 532, 435–437.
2.   L. Moura, C. C. Santini and M. F. Costa Gomes, *Oil Gas Sci. Technol. – Rev. d'IFP Energies Nouv.*, 2016, **71**, 23.
3.   C. Hardacre, J. D. Holbrey, C. L. Mullan, M. Nieuwenhuyzen, T. G. A. Youngs, D. T. Bowron and S. J. Teat, Phys. Chem. Chem. Phys., 2010, **12**, 1842–1853.
4.   J. Estager, J. D. Holbrey and M. Swadźba-Kwaśny, *Chem. Soc. Rev.*, 2014, **43**, 847–886.
5.   M. He, S. Liu, L. Bai and X. Liu, *Chem. Eng. Res. Des.*, 2018, **137**, 186–193.

QUILL Quarterly Report

February 2022 – April 2022

Name:	Emma McCrea
Supervisor(s):	Prof Gosia Swadzba-Kwasny and Prof John Holbrey
Position:	PhD student
Start date:	1/10/21

Start date:	1/10/21	Anticipated end date:	30/9/24
Funding body:	EPSRC		

Acidic Ionic Liquids As Catalysts For The Valorisation Of Waste Plastic Resource

In this project, the chemical recycling of waste plastic feedstock will be investigated with the use of liquid coordination complexes and ionic liquids as Lewis acid catalysts. The aim is to develop an inexpensive acidic ionic liquid catalyst that can function with highly contaminated feedstocks. The oligomerisation of olefins will transform the feedstock into lubricating base oil which is used in a range automotive machine to improve efficiency.

1.
- Research into literature focusing on liquid coordination complexes, borenium ionic liquids and oligomerization of olefins to base oils.

2.
- Synthesis of 2 borenium ionic liquids: $[BCl_2(py)][Al_2Cl_7]$ and $[BCl_2(4pic)][Al_2Cl_7]$.
- Synthesis of 2 liquid coordination complexes: Ur-$AlCl_3$ and $P_{888}O$ -$AlCl_3$
- Oligomerization of 1-decene with 4 catalyst mentioned above and analysis of product stream.
- Oligomerization of waste feedstock with analysis of product stream
- Purification of waste feedstock stream before oligomerization.

3.
- Create a matrix of catalyts at different loading with emphasis on ambient and mild conditions.
- apply matrix to purified feedstock and analyse product stream
- Optimisation of reaction conditions

QUILL Quarterly Report

February 2022 – April 2022

Name:	Anne McGrogan		
Supervisor(s):	Prof Gosia Swadzba-Kwasny		
Position:	PhD		
Start date:	01/10/2019	Anticipated end date:	31/03/2023
Funding body:	EPSRC		

Boron Lewis Acids: Structure and Applications

Background

Many boron compounds are Lewis acidic, either due to the presence of a free p orbital in species with sp^2-hybridised boron, or due to labile ligands attached to sp^3-hybridised boron that can be readily replaced by a nucleophile.[1] Quantifying Lewis acidity of these various boron compounds is very challenging, which to a certain extent hinders understanding of their reactivity.
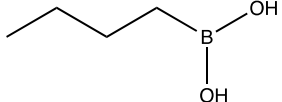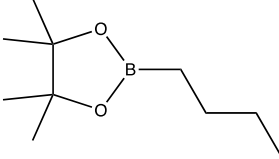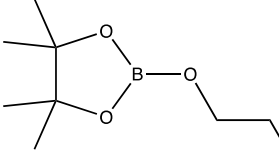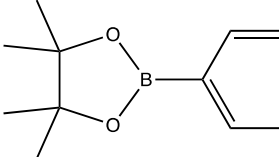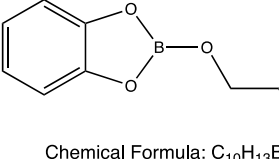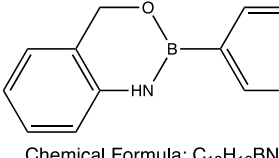
Our group has a long-standing interest in Lewis acidic ionic liquids, which has led us to the development of ionic liquids with tricoordinate, Lewis superacidic borenium cations.[1] Their acidity was quantified using the Gutmann acceptor number,[2] the most common method for probing Lewis acidity of ionic liquids. However, as a method based on a ^{31}P NMR spectroscopic probe (triethylphosphine oxide), Gutmann's approach is necessarily dependent on hard-soft acid-base (HSAB) explanations. Lewis acidity is measured against a single base and it is not sufficient to compare compounds of widely differing Lewis acidities. It does not give insight into different factors influencing Lewis acidity: hardness/softness of acid/base in a Lewis adduct, electronic environment of boron, energy required to alter geometry around the boron centre upon the adduct formation.

In this work we have set out to study directly the electronic environment of boron using liquid jet X-ray photoelectron spectroscopy (XPS). Boron 1s X-ray spectroscopy is not commonly measured due to extensive experimental challenges, especially in the liquid phase. This technique does not require the probe and is very much complementary to the Gutmann's method. By understanding how the electronic structure relates to chemical reactivity and probe-based Lewis acidity measurements, we aim to elucidate different factors that influence Lewis acidity, and understand how each impacts the catalytic performance of boron Lewis acids.

Progress to date

The experiments were performed at the BESSY II synchrotron, Berlin, using a combination of liquid-jet sample delivery with XPS, resonant XPS and X-ray absorption spectroscopy (XAS). Six boron compounds were studied (Table 1).

Table 1 - Boron compounds studied by XPS at the at the BESSY II synchrotron, Berlin.

Sample	Code Name	Lab book name	Chemical formula/Structure
1	Butylboronic acid	Butylboronic acid	Chemical Formula: $C_4H_{11}BO_2$ Molecular Weight: 101.94
2	B(pin)(Bu)	Butyl boronic acid pinacol ester	Chemical Formula: $C_{10}H_{21}BO_2$ Molecular Weight: 184.09
3	B(pin)(OBu)	Butyl borate pinacol ester	Chemical Formula: $C_{10}H_{21}BO_3$ Molecular Weight: 200.09
4	PhB(pin)	Phenylboronic acid pinacol ester	Chemical Formula: $C_{12}H_{17}BO_2$ Molecular Weight: 204.08
5	B(cat)(OBu)	Butyl borate catechol ester	Chemical Formula: $C_{10}H_{13}BO_3$ Molecular Weight: 192.02
6	PhB(C7H9NO)	Phenyl boronic acid 2-amino benzyl alcohol ester	Chemical Formula: $C_{13}H_{12}BNO$ Molecular Weight: 209.06

B 1s XAS was recorded to identify the boron-based unoccupied molecular orbitals (Mos). A single peak is observed in the spectra (Figure 1), due to one π^* unoccupied valence state. The peak energy gives the energy for the transition from the B 1s to the empty B p orbital, so effectively the energy of the LUMO of the boron. A lower LUMO energy would translate into a greater Lewis acid as the boron would more readily accept electrons. The peak energy varies greatly with structure, up to 3 ev. This demonstrates that structure has a large effect on the B 1s $\rightarrow \pi^*$ energy. A larger B 1s $\rightarrow \pi^*$ energy is observed for compounds with 3 B-O bonds. Ongoing analysis of the results but preliminary results validate the new approach of measuring boron 1s X-ray spectroscopy to provide insight into Lewis acidity of tricoordinate compounds of boron.
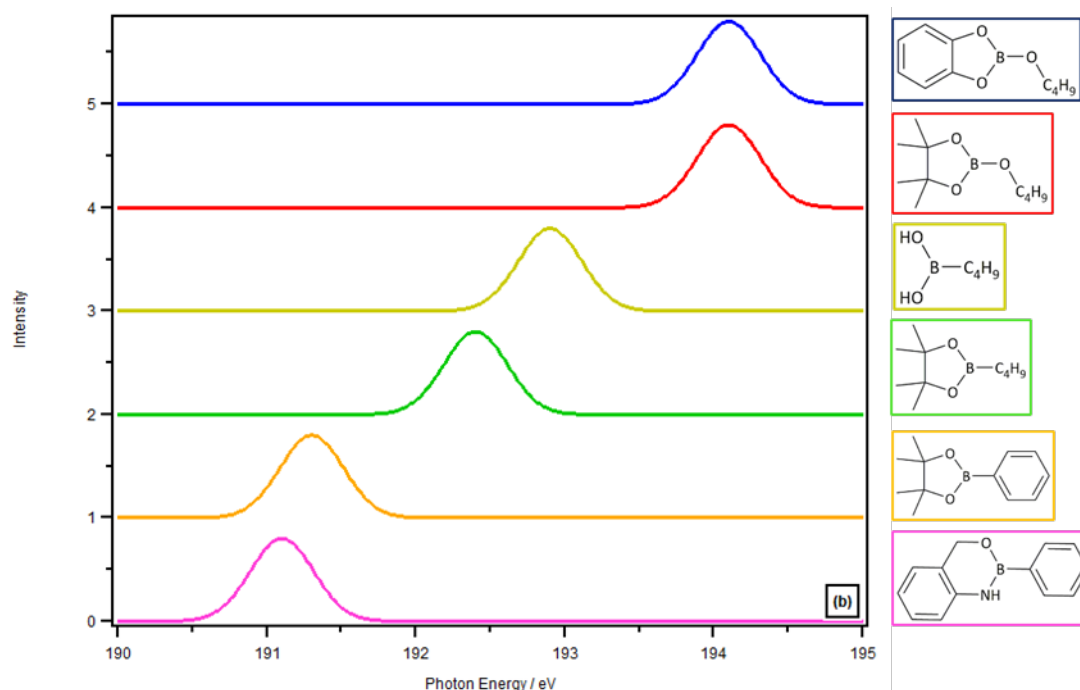
Figure 1 - Boron 1s XAS data for the six boron compounds studied.

Time-dependent DFT calculations of B 1s XAS were carried out by collaborator Tom Penfold from University of Newcastle. Very good linear correlation is observed between experimental and calculated B 1s → π* energies, which validates both our experiments and calculations (Figure 2).

y = 1.09x - 26.05
R^2 = 0.97
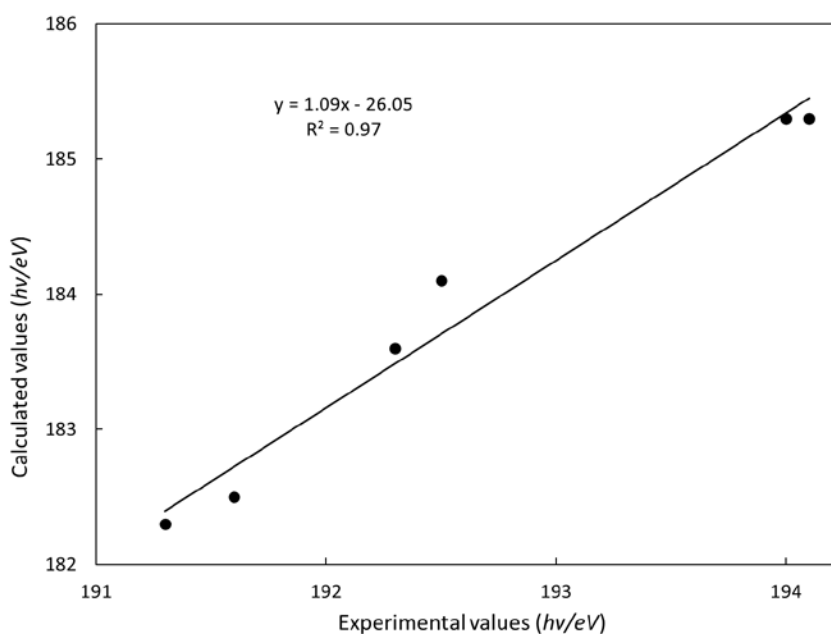
Figure 2 - Calculated vs experimental B 1s XAS values (hv/ev)

I have also been synthesising deuterated compounds for two neutron scattering experiments at the Rutherford Appleton Laboratory at ISIS neutron and muon source, Oxfordshire. As well as analysing previous neutron scattering data using Dissolve software.

Conclusions and future work

Preliminary results validate the new approach of measuring boron 1s X-ray spectroscopy to provide insight into Lewis acidity of tricoordinate compounds of boron. Future work will involve continued analysis and interpretation of data.

References

1.   S. Coffie, J. M. Hogg, L. Cailler, A. Ferrer-Ugalde, R. W. Murphy, J. D. Holbrey, F. Coleman and M. Swadźba-Kwaśny, *Angew. Chem. Int. Ed.*, 2015, **54**, 14970–14973.
2.   V. Gutmann, *Electrochim. Acta*, 1976, **21**, 661–670.

Name:	Shannon McLaughlin		
Supervisor(s):	Prof Gosia Swadźba-Kwaśny		
Position:	PhD Student (2nd year)		
Start date:	October 2020	Anticipated end date:	July 2024
Funding body:	Department for the Economy		

Thinking Inside the (Glove)Box: Lewis Superacidic Ionic Liquids Based on Main Group Cations

Background

The chemistry of Lewis acidic main group cations is of increasing importance, as metal-free catalysis gains interest of the scientific community. One of the longest-standing challenges in main group synthetic chemistry has been the preparation of tricoordinate, tetravalent silicon cations in the condensed phase. Silylium ions are extremely Lewis acidic and have a high electrophilicity, oxophilicity and fluorophilicity, affording unique transformations that cannot be performed by traditional metal catalysts. Recently, synthetic methods to generate stable silylium cations have become more accessible and more effective.

Silylium ions can be categorised as either stabilised or 'free' (Figure 1a). As they are highly reactive, silicon cations are commonly found as species which are stabilised, whereas 'free' silicon cations are extremely rare. The first ever 'free' silylium cation to be isolated was the trimesitylsilylium cation (($Mes)_3Si^+$) illustrated in Figure 1b.[1] Silylium ions are usually quite a reactive species but the bulky mesityl groups in compound **1** help to shield the silicon centre from attack by large nucleophiles. These steric interactions also prevent the silylium ion reacting with the solvent and the product alkene making it much more stable. The tridurylsilylium cation (($duryl)Si^+$)[2] was later isolated along with the related species ($C_6Me_5)_3Si^+$.[3] Till date these three compounds are the only examples of 'free' species whose structures have been confirmed by X-ray crystallography.

σ-Donor stabilised

π-Donor stabilised

'free' (unstabilised)

$[B(C_6F_5)]^-$

1
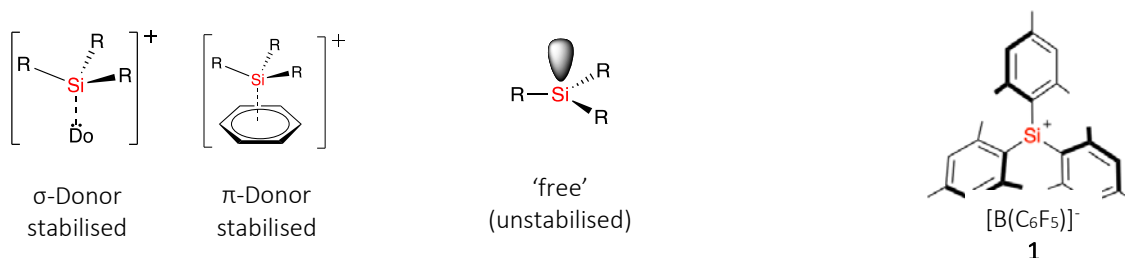
Figure 1 - a) Example structures of stabilised and unstabilised silylium

b) Structure of 'free' trimesitylsilylium cation.

Objective

This work reports on the first-ever attempt to prepare and characterise silylium ionic liquids.

The first goal of this project is to synthesise the 'free' trimesitylsilylium cation. The synthesis of trimesitylsilane, chlorotrimesitylsilane, and allyltrimesitylsilane will follow methods described by Lappert et al.,[4] Zigler et al.[5] and Lambert and Zhao,[6] respectively. The allyltrimesitylsilane will be used to synthesise the 'free' trimesitylsilylium cation following the method described by Lambert et al.[1]

The 'free' trimesitylsilylium cation will then be combined with non-coordinating anions, such as $[B(C_6F_5)]^-$ (compound **1**), $[NTf_2]^-$ and $[eFAP]^-$ to conduct characteristic studies.

Synthesis of Allyltrimesitylsilane:
Previous work involved the successful synthesis of trimesitylsilane and chlorotrimesitylsilane which is described in detail in previous reports. The synthesis of allyltrimesitylsilane is illustrated in Scheme 1 and Figure 2.
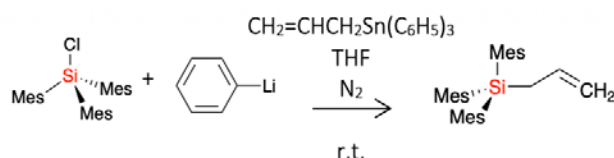
Scheme 1 - Synthesis of allyltrimesitylsilane.
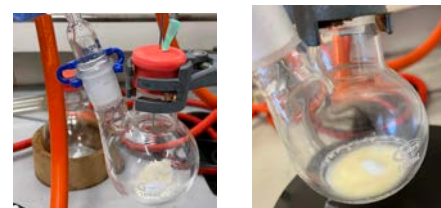
Figure 2 - a) Cannula transfer of allyllithium (left) to chlorotrimesitylsilane (right).

b) Crude mixture of allyltrimesitylsilane.

Phenyllithium solution was quickly added to a round bottom flask containing anhydrous tetrahydrofuran (THF) and allyltriphenyltin in a under argon. This generated allyllithium along with a precipitate of tetraphenyltin (Ph_4Sn). The suspension was transferred into a round bottom flask containing chlorotrimesitylsilane using cannula filtration. The reaction mixture was stirred at room temperature for two days until all the chlorotrimesitylsilane has reacted. Final work-up and purification steps of the allyltrimesitylsilane are yet to be completed. Crude solution will be extracted with hexane, dried over $MgSO_4$, concentrated *via* rotary evaporation, and chromatographed over silica gel using hexane as the eluent. ^1H and ^{13}C NMRs of the allyltrimesitylsilane (white solid) will be ran in deuterated benzene (C_6D_6) and a ^{29}Si NMR will be ran in deuterated chloroform ($CDCl_3$).

Alternative Synthetic Route:
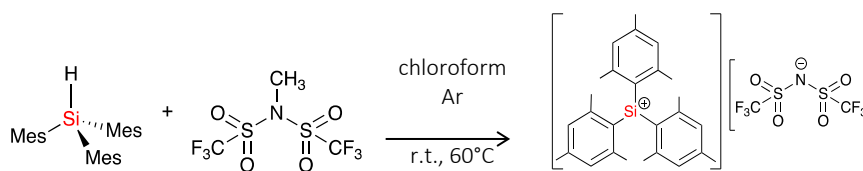
Scheme 2 - Synthesis of trimesitylsilylium bis(trifluoromethanesulfonyl)imide [(Mes)$_3$Si][NTf$_2$].

Figure 3 - [(Mes)$_3$Si][NTf$_2$] crystals.

A novel synthetic route, illustrated in Scheme 2, was prosed to generate trimesitylsilylium bis(trifluoromethanesulfonyl)imide [(Mes)$_3$Si][NTf$_2$] (Figure 3). The trimesitylsilane starting material was synthesised following the method described previously by Lappert et al.[4] Trimesitylsilane was allowed to react with n-methyl bis[(trifluoromethyl)sulfonyl]imide

(Me[NTf$_2$]) in chloroform and the resulting mixture was set to reflux at 50°C under argon for two days. The solvent was removed *via* rotary evaporation which left a pale-yellow viscous liquid. ^{1}H, ^{13}C and ^{29}Si NMRs of this liquid were ran in CDCl$_3$. The ^{1}H NMR (Figure 4) showed a peak at 5.78 ppm which confirmed that there was still some unreacted trimesitylsilane remaining. This peak is due to the hydrogen bonded directly to the silicon centre in trimesitylsilane, this signal should disappear once all the starting material has been converted to chlorotrimesitylsilane. This mixture was then dissolved in acetonitrile solvent and the solution was set to reflux at 60°C for a further 2 days. The new solvent was chosen due to its higher boiling point. This allowed the mixture to be refluxed at a higher temperature and helped drive the reaction to completion. When the new solvent was removed *via* rotary evaporation white crystals formed suggesting that an adduct had formed with the acetonitrile. ^{1}H, ^{13}C and ^{29}Si NMRs of these crystals were recorded in CDCl$_3$. NMRs confirmed the successful synthesis of trimesitylsilylium bis(trifluoromethanesulfonyl)imide [(Mes)$_3$Si][NTf$_2$].

Figure 4 - ^{1}H NMR spectrum of in CDCl$_3$.
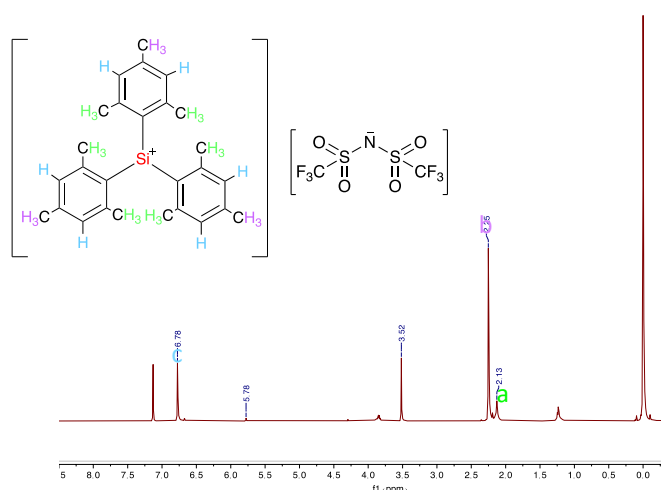
Characteristic studies

The crystals of [(Mes)$_3$Si][NTf$_2$] obtained from the reaction in Scheme 2 were characterised using multiple analytical techniques, including thermogravimetric analysis (TGA), differential scanning calorimetry (DSC) and single crystal x-ray diffraction (XRD).
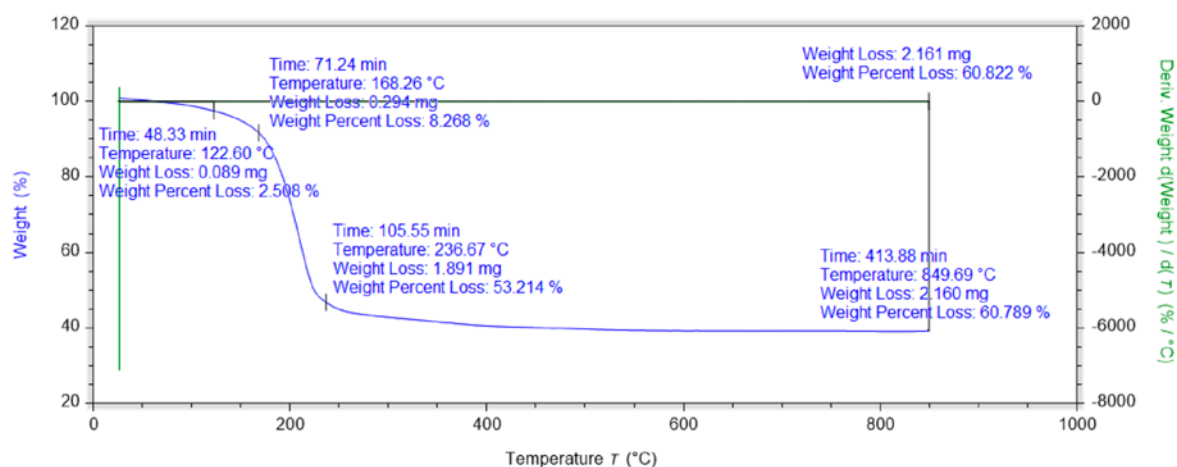
Thermogravimetric Analysis:

Figure 5 - TGA curve of [(Mes)$_3$Si][NTf$_2$].

Thermogravimetric analysis of [(Mes)$_3$Si][NTf$_2$] was conducted to determine its thermal stability. The TGA curve (Figure 5) shows that the onset temperature occurs at 168.3 ˚C. The onset temperature is the temperature at which the compound first starts to decompose. There was a weight percentage loss of 45.0% between 168.3 ˚C and 236.7 ˚C. At 850 ˚C there was approximately 40% of my sample by weight remaining which suggests the compound is very stable. As the sample did not fully decompose the endset temperature was unable to be determined. A second sample of [(Mes)$_3$Si][NTf$_2$] will be submitted for TGA using ceramic pan instead of platinum. This will allow the compound to be heated to a much higher temperature (<1200 ˚C) and ensure complete decomposition.

Differential scanning calorimetry

The DSC curve of [(Mes)$_3$Si][NTf$_2$] (Figure 6) shows the melting point (endothermic peak) and crystallisation (exothermic peak). The melting point occurs at 113.1 ˚C. Crystallisation begins at -18.6 ˚C and ends at -20.9 ˚C, this indicates that the glass transition temperature occurs at -20.4 ˚C, which is the midpoint between these two values. The endothermic peak is broad which suggests that melting occurs slowly whereas the exothermic peak is flat suggesting that crystallisation occurs much more quickly. The rapid crystallisation of the sample indicates that [(Mes)$_3$Si][NTf$_2$] prefers to arrange itself in a crystalline order rather than in an amorphous state.
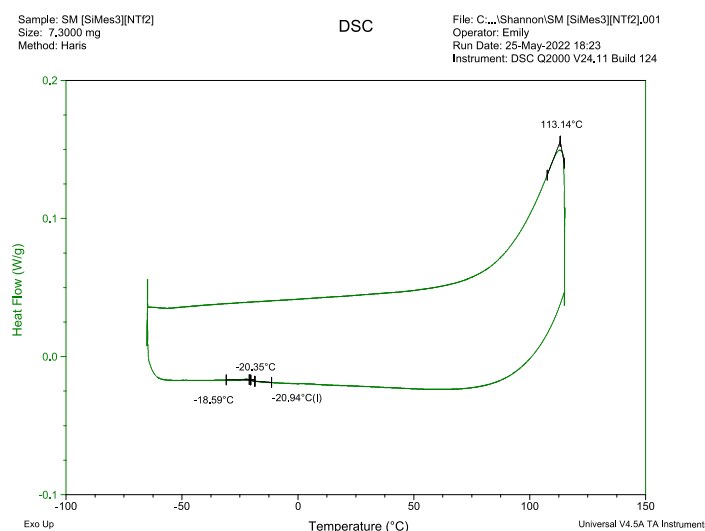
Figure 6 - DSC curve of [(Mes)$_3$Si][NTf$_2$].

Single crystal X-ray diffraction

A crystal of [(Mes)$_3$Si][NTf$_2$] was submitted for variable temperature single crystal XRD. The results showed that there were multiple layers in the sample chosen which caused disorder and prevented a clear crystal structure from being obtained. [(Mes)$_3$Si][NTf$_2$] will be recrystallised *via* slow evaporation or vapour diffusion and a new sample will be submitted for both single crystal and powder X-Ray diffraction. Powder XRD will help to determine whether the crystal structure is representative of the bulk of the sample.

Conclusions and future work

This work confirms the successful synthesis of trimesitylsilylium bis(trifluoro-methanesulfonyl)imide [(Mes)$_3$Si][NTf$_2$] using a novel synthetic procedure. The crystal sample obtained will be recrystallised and submitted for further characterisation. A repeat TGA will be run to calculate the endset temperature and sample will be submitted single crystal and powder XRD to determine the crystal structure. This reaction will also be repeated using chloroform as the solvent to regenerate the liquid that formed initially. Future characteristic studies of this liquid will be conducted, including TGA and DSC.

Future work will also involve completing the final steps of the proposed synthesis of the 'free' trimesitylsilylium cation.

Allyltrimesitylsilane will be purified and trimesitylsilylium tetrakis(pentafluorophenyl)borate (compound **1**) will be synthesised. An allyl leaving group method is used to generate the free silicon cation and the corresponding alkene. The driving force for this reaction is provided by the relief of steric strain around the original tetracoordinate silicon centre. These salts are difficult to crystallise properly and instead they tend to form oils or liquid clathrates.[1] Therefore, there is a potential to use these materials for unique applications such as ionic liquids.

After compound **1** has been successfully synthesised, it will be combined with commonly used anions such as [B(C$_6$F$_5$)]$^-$, [NTf$_2$]$^-$, [FSI]$^-$ and [eFAP]$^-$ to conduct characteristic studies of the cation. The next aim would be to combine the trimesitylsilylium cation with borate anions or cyanoborate anions in hope of generating new Lewis superacidic ionic liquids. Applications of these newly developed ionic liquids will then be investigated for potential use as solvents and catalysts.

References

1. K. C. Kim, C. A. Reed, D. W. Elliott, L. J. Mueller, F. Tham, L. Lin and J. B. Lambert, *Science.*, 2002, **297**, 825–827.
2. J. B. Lambert and L. Lin, 2001, J. Org. Chem., 66, 8537–8539.
3. A. Schäfer, M. Reißmann, S. Jung, A. Schäfer, W. Saak, E. Brendler and T. Müller, 2013, Organometallics, **32**, 4713-4722.
4. M. J. S. Gynane, M. F. Lappert, P. I. Riley, P. Rivière and M. Rivière-Baudet, J. Organomet. Chem., 1980, **202**, 5-12.
5. S. Zigler, L. M. Johnson and R. West, J. Organomet. Chem., 1988, **341**, 187-198.
6. J. B. Lambert, C. L. Stern, Y. Zhao, W. C. Tse, C. E. Shawl, K. T. Lentz and L. Kania, J. Organomet. Chem., 1998, **568**, 21-31.
7. M. Gynane, M. Lappert, P. Riley, P. Rivière and M. Rivière-Baudet, Journal of Organometallic Chemistry, 1980, **202**, 5-12.
8. S. Zigler, L. Johnson and R. West, Journal of Organometallic Chemistry, 1988, **341**, 187-198.
9. J. Lambert, C. Stern, Y. Zhao, W. Tse, C. Shawl, K. Lentz and L. Kania, Journal of Organometallic Chemistry, 1998, **568**, 21-31.

QUILL Quarterly Report

February 2022 – April 2022

Name:	Hugh O'Connor		
Supervisor(s):	Prof Peter Nockemann, Dr Stephen Glover and Dr Josh Bailey		
Position:	PhD Student		
Start date:	October 2019	Anticipated end date:	June 2023
Funding body:	EPSRC		

Redox Flow Battery Materials for Energy Storage

Background

As fossil fuel supplies dwindle and the climate change problem escalates, the need to harness renewable energy resources increases. However, these energy sources are intermittent and unpredictable, making them difficult to be used in a safe and stable power grid. For this reason, it is important that new energy storage technologies are developed which can shift energy from off-peak demand times to peak demand times. One of the most promising emerging technologies is the redox flow battery (RFB).

In RFBs, redox couples are dissolved in electrolyte solutions and stored in separate reservoir tanks. During charge and discharge these electrolytes are pumped from reservoir tanks into half cells where they react in an electrode, either consuming or generating electrons.

This working principle gives rise to a number of key advantages over other conventional battery technologies. In flow batteries, power and energy is decoupled; power is controlled by the stack effectiveness whilst energy is stored in the electrolyte reservoir tanks. This makes RFBs highly customisable, allowing them to be tailored to meet the demands of various power grids. They also have a long working life; with the electrolytes stored in separate tanks, the electrodes don't undergo complex redox reactions and experience less structural changes and strain than those found in conventional batteries. One drawback of RFBs however is their low energy density and high costs when compared to other energy storage technologies.

Improving the energy density, energy storage efficiency and sustainability could make RFBs an even more promising candidate for large scale energy storage applications. Innovative and more efficient manufacturing techniques could also potentially provide a solution in reducing inevitable costs that will occur when implementing a new energy storage technology.

One method of improving the performance of RFBs is designing better performing flow fields, manifolds and cell stack topologies resulting in a better performing cell stack

Objective of this work

To investigate the effect of modified cell topology and stack architecture on the power density of redox flow batteries, identifying key performance influencers and improving economic viability.

Progress to date

Extensive work has been carried out into the investigation of novel cell and manifold topologies to improve cell performance. Fused Deposition Modelling (FDM) 3D-printing has been identified as a powerful tool to produce lab scale RFB test cells at an extremely low cost. At the end of the previous quarter, these findings were published in a paper for the RSC journal Sustainable energy and fuels. In the subsequent months, this platform has been used to evaluate new, novel cell topologies, to probe the effect changes have on cell performance. Expansion of testing capacity has also been completed to expedite this work, allowing four flow battery systems to be tested simultaneously. This has also facilitated the development of new novel electrolytes for low cost energy storage. Lastly, the 3D-printing platform has been used to manufacture miniaturised flow cells for micro X-ray CT imaging in the synchrotron at diamond light source. This work has yielded interesting results into the interaction between electrolyte and different electrodes within flow battery cells. Data analysis on these images are ongoing and will be complete in the coming months.

Conclusions and future work

FDM 3D-printing has proven an invaluable tool in producing fully customisable low-cost test cells in order to allow for the development of new cell topologies and materials. The platform developed is being utilised and expanded to further research into novel electrolyte technologies, research into electrolyte/ electrode interaction and flow cell design.

QUILL Quarterly Report

February 2022 – April 2022

Name:	Liam O'Connor		
Supervisor(s):	Dr O Istrate and Prof B Chen		
Position:	PhD student		
Start date:	01st Oct 2019	Anticipated end date:	30th Sept 2023
Funding body:	Department for the Economy		

3D-Printed Polymer Graphene Nanocomposites for Biosensor Applications

Background

A polymer strain sensor works on the principle that the electrical conductivity is proportional to the mechanical strain applied. Thus far, literature has focused on the prosthetic using feedback from pressure sensors in the fingertip to give feedback to the user. One of the limitations of using this pressure sensor is that it can only distinguish objects within the surface area of the sensors, which is 15 mm2. A solution to the limitation of pressure sensors is to develop a strain-dependent electrically conducting material and coat the outer material of the prosthetic. An important feature of the material used to manufacture a prosthetic arm is that it needs to be 3D printable. 3D printing of the prosthetic arm is required because there is not a standard size for a person's arm. The materials being investigated are thermoplastic polyurethane (TPU) because of its strong hysteresis response to mechanical strain, nylon-11 (PA11) because of its piezoelectric properties, and graphene nanoplatelets (GNP) because it is shown to increase the electrical conductivity of other piezoelectric polymers, such as polyvinylidene fluoride (PVDF) at 25 wt.% (weight per cent)

Objective of this work

The objective of the work is to develop a strain-dependent electrically conducting material that could be used as a strain sensor and can be FDM 3D printed. This will be done by determining the optimal graphene for the manufacturing of TPU/GNP filaments, determining the optimal graphene loading for the manufacturing of PA11/GNP filaments, determining the optimal graphene loading for the manufacturing of TPU/PA11/GNP filaments, and determining the optimal manufacturing layering for TPU/PA11/GNP filaments.

Progress to date

Characterisation of the PA11 nanocomposite has shown that the GNPs are attracted to the hydrogen bonds within the PA11. This attraction of the GNPs to the hydrogen bonds prevents the polymer chains from sliding and rapidly decreases the elongation at break. An electrical percolation threshold was found at 7.9% wt. % and a rheological percolation threshold was found at 9.3 wt. % which suggests that there is a soft and rigid percolation threshold occurring within the. The TPU/PA11/GNP nanocomposite has been mixed with a TPU/PA11 ratio of 70/30 and a GNP loading of 2.5, 5, 7.5, and 10wt. % and are waiting to be extruded

Conclusions and future work

The next stage of the project is to manufacture the TPU/PA11/GNP nanocomposite and thermally, mechanically and electrically characterise the material.

QUILL Quarterly Report

February 2022 – April 2022

Name:	Scott Place		
Supervisor(s):	Dr Paul Kavanagh (Primary) and Dr Mark Muldoon (Secondary)		
Position:	PhD Student		
Start date:	Oct 2019	Anticipated end date:	Jul 2023
Funding body:	EPSRC		

Molecular Electrocatalysts for Energy and Electrosynthetic Applications

Background

This project focuses on the nitroxide radical molecule TEMPO and its derivates, their electrokinetic properties, and their applications in energy storage, energy generation, and electrosynthetic applications. TEMPO-like molecules are able to be electrochemically oxidised at an electrode surface to an active oxoammonium form, which can then react with substrates in a chemical redox reaction, which regenerates them to their nitroxide (or hydroxide, when protons are present) form. These reactions follow the well-established EC' (electrochemical-chemical) two-step reaction profile, studied extensively by Savéant and co-workers and Dempsey and co-workers, among others.

Electrolysis for organic synthesis is gaining popularity in the literature as a low-waste and simple procedure for converting a number of substrates to their corresponding products. TEMPO and its derivatives are an example of chemicals that can be used as electrocatalysts for oxidation reactions, where direct electrochemical oxidation of the substrate may be too energy-intensive.

Objective of this work

In this part of the study, we aim to use the TEMPO-mediated oxidation of benzyl alcohol as a benchmarking case study, where develop an electrochemical method of catalyst benchmarking in a synthetic context. Many organic chemists have had little exposure to electrochemistry in their careers, and may find some of the calculations, rate constants, and other electrochemical parameters unclear. We aim to develop a straightforward method of electrochemical catalyst benchmarking (using such techniques as cyclic voltammetry and chronoamperometry) and elucidate the relationship between calculated electrochemical parameters and their usefulness in organic synthesis. Similar efforts have been made in the context of catalyst benchmarking for hydrogen generation for the energy industry, but none in the context of organic synthesis.

Progress to date

In the previous report, I detailed my work on establishing pseudo-first order conditions for applying the Savéant framework for the benchmarking of molecular electrocatalysts. These sort of studies provide a wealth of useful kinetic information, but may miss important details

such as catalyst stability / selectivity. The last few months have been focused more on applying these reaction conditions to much longer-term studies, on the order of 4-8 hours, as opposed to 15 seconds. These so-called chronoamperometric (CA) studies allow us to monitor the kinetic performance of a catalyst in real time by measuring current. By integrating these traces, we can determine how much charge has been passed in the experiment, and thus our expected conversion of substrate to product in our oxidation reaction. There have been significant challenges along the way with regard to obtaining reproducibility in these experiments, as the setup can be fiddly (distance deltas of a few millimetres between electrodes across different experiments can have enormous consequences on observed current). But cell setup now seems to be optimised to obtain allowable results. We attempted to couple these experiments with NMR and HPLC analysis of our product mixtures, but determined that NMR was too insensitive for this purpose, and wouldn't give us any idea of any overoxidation to carboxylic acids, as carboxylic acids can be very difficult to detect by NMR. HPLC was incompatible with tis reaction system due to large quantities of base used and insensitivity of HPLC to benzaldehyde. More recently, in the past few weeks, I have been working with Dr Mark Muldoon's team to employ Gas Chromatography (GC) for this purpose, which appears more promising. This week, we determined seemingly optimal conditions for GC, and are beginning to apply it to real product mixtures.

Conclusions and future work

Reaction conditions and analytical parameters have been optimised and work is underway to produce a final set of data for a number of different TEMPO-based catalysts. The next two/three weeks will be focused on generating product mixtures using various catalysts from long-term electrolysis experiments and submitting them for GC analysis to determine conversion rates, yields, and mass balance.

QUILL Quarterly Report

February 2022 – April 2022

Name:	Junzhe Quan		
Supervisor(s):	Prof John Holbrey and Dr Leila Moura		
Position:	PhD		
Start date:	01/10/2019	Anticipated end date:	01/10/2023
Funding body:	Self funding		

Use Ionic liquids That Exhibit LCST (Lower Critical Solution Temperature) Behaviour as Draw Fluids for Water Treatment, Desalination and Separation

Background

New Ionic liquid materials have been recently developed that exhibit lower critical solubility temperature (LCST) behaviour with water, that is, they are miscible at a low temperature and split into two aqueous phases on heating beyond a critical temperature. Such materials have the potential to be used as draw fluids for forward osmosis (FO) water desalination using low grade energy to address the global challenge to provide clean, accessible drinking water to all the world's populations. In this research programme, new ionic liquids will be investigated as advanced fluids for forward osmosis water treatment. This offers opportunities to advance less energy intensive alternative to conventional reverse osmosis as a solution to the global challenge of providing potable water in regions of low availability.

Objective of this work

My research program in the use of ionic liquids as potential draw fluids for FO water treatment includes:

1. Preparation of appropriate model ionic liquids
2. Characterisation of aqueous/ionic liquid phase behaviour as a function of aqueous component salinity, pH, temperature and to draw structure-performance relationships with the ionic liquid cation/anion components.
3. Develop a FO membrane cell to test and evaluate draw fluid characteristics and parameters of selected systems.
4. Optimize ionic liquid to use as draw fluid, developing a proof-of-concept ionic liquid-based FO desalination demonstrator for benchmarking
5. Examine the applicability of these draw fluids to water-processing of a range of feeds and product streams (desalination, waste concentration, biomass dewatering).
6. Measure the energy consumption and compare with typical method of water treatment

Progress to date

The third ionic liquid tetrabutylphosphonium p-toluenesulfonate was tested by Crystal16 for LCST. Its data was attached to the phase diagram.

Salt Concentration(g/L)	0	20	30	40	50
Cloud points temperature (°C) of 50% mass fraction TsO/salt solution mixtures	19.0	15.6	13.4	11.9	10.2

Table 1 - Cloud points of [P$_{4444}$][TsO]
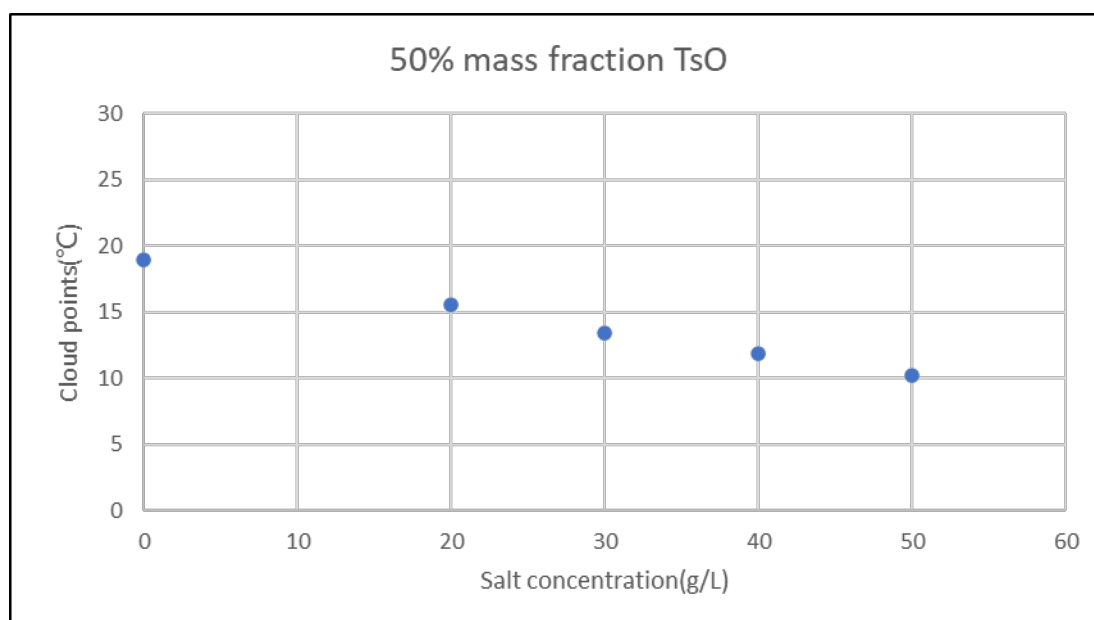
Figure 1 - Cloud points of [P$_{4444}$][TsO]under different salt concentration in 50% mass fraction IL concentration
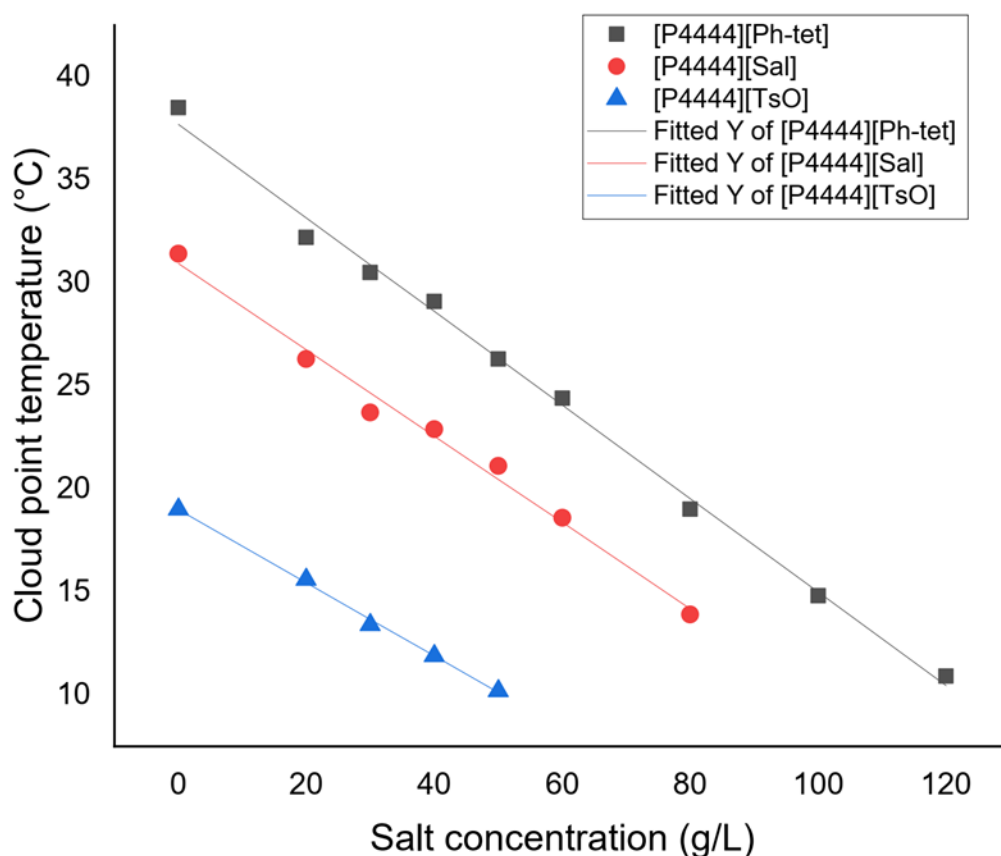
Figure 2 - Comparison and contrast between [P$_{4444}$][Ph-tet], [P$_{4444}$][Sal] and [P$_{4444}$][TsO]

Conclusions and future work

It provides an important auxiliary role for us to calculate and predict the lower critical solution temperature change during the separation process. The figure shows us that IL/water system has a downtrend when the salt concentration increase. It suggests that high salinity decrease the hydrophilicity of ionic liquids resulting in the LCST phase behaviour occurring in lower temperature. It will give full theoretical support to the concept of IL applying for forward osmosis. We can use this characteristic to graded desalination. The next step is to set up and run a lab-scale forward osmosis test system.

QUILL Quarterly Report

February 2022 – April 2022

Name:	Richard Woodfield		
Supervisor(s):	Dr Stephen Glover, Dr Robert Watson and Prof Peter Nockemann		
Position:	PhD Student		
Start date:	06/2019	Anticipated end date:	12/2022
Funding body:	EPSRC		

Modelling the use of Flow Batteries in Transport Applications

Background

Flow batteries have received significant attention in the past years for use in grid storage applications. The decoupling of the relationship between power and energy density offers a very unique way to store energy to suit the user's particular needs. The extremely long cycle life of a flow-battery is another attractive asset, as the electrodes do not undergo cyclic stressing in the same way Li-ion and other chemistries do. Flow-batteries have received very limited attention regarding their use in transport applications. There is untapped potential in the fact that the discharged electrolyte of a flow-battery could be rapidly swapped at a traditional gas-station, where the infrastructure is already half in-place with storage tanks under the stations. With the electrolyte being entirely re-usable, the station would use an on-site flow-battery to recharge their reservoir and provide passing vehicles with opportunity to swap their electrolyte with readily charged fluid.

Objective of this work

The overall goal of the project is to identify viable electric or hybrid modes of transport that would benefit from the use of a flow-battery, given the refillable nature of the flow-battery electrolyte reservoirs. Even the applications rendered not viable will have outcomes, as the amount by which the energy density of the electrolyte would need to improve by is also providing electrolyte chemists with targets to aim for. The investigations will be carried out using software to model battery and vehicle behaviour, primarily Simulink.

Progress to date

The modelling work has revealed that coastal ferries show great potential for the application of vanadium redox flow-batteries. The use case explores a scenario where the ferry travels between two ports, each of which have a large vanadium redox flow-battery powered by the grid. The ferry can then rapidly swap depleted electrolyte with the port batteries. A paper covering this work has been submitted to the Journal of Energy Storage.

The focus of the project has now shifted toward bus transport. Since redox flow batteries have low energy density, a pure vanadium redox flow battery bus is non-viable. Li-ion, vehicle, PEMFC, and cabin temperature models have been developed in parallel, which will come together with the existing redox flow battery models to explore the energy management of a redox flow-battery bus using real-world bus driving data and standard driving cycles.

Conclusions and future work

A paper has been published in the area of redox flow-battery ferries, and future work will investigate the viability of coupling various technologies with redox flow-batteries in buses. A full investigation into the optimization, running costs, and life-cycle implications will be conducted. Vanadium redox flow-batteries have great potential to bring down the cost per year of ownership due to their long life-span, while offering a method of recharging rapidly. It is thought that the flow-battery with its fast dynamic response may pair very well with PEMFC technology, which has inherently bad dynamic response.

QUILL Quarterly Report

February 2022 – April 2022

Name:	John Young		
Supervisor(s):	Dr Leila Moura, Prof John Holbrey and Prof Sophie Fourmentin		
Position:	PhD student		
Start date:	2020	Anticipated end date:	2024
Funding body:	EPSRC		

Gas Separation Technologies

Background

Biogas is a renewable and carbon neutral energy source obtained through anaerobic digestion (AD) of organic waste. Biomethane is obtained through the upgrading of biogas produced from anaerobic digesters. It consists of mainly methane and carbon dioxide with many trace compounds including hydrogen sulfide, ammonia, silioxanes, terpenes and water vapour. Biomethane must be of a purity equal to or better than that of natural gas if it to be utilised for grid injection therefore a methane purity of above 96% must be achievable from any prospective technology. Carbon dioxide should make up 2.5-4% of the remaining volume with contaminants such as sulfur and siloxanes being limited to 10 mg/m^3 and 0.1 mg/m^3 respectively. The primary focus of this research is on carbon dioxide/methane separation as these are the two major components of biogas.[1]

Currently biogas upgrading is multistep, with scrubbing used for carbon dioxide removal from the biogas stream to concentrate methane. This involves the use of liquid amines such as MEA (monoethanolamine) where carbon dioxide is captured through a chemisorption process. Regeneration of the amines requires high energy inputs in the form of steam at 100-150°C to reform the initial liquid amine. Water scrubbing can also be used but this requires large amounts of water and leads to methane slip due to the lower selectivity of water compared with other technologies. Membranes offer another option for upgrading but these also suffer from a range of issues such a low throughput coupled with fouling and plasticisation. The degradation of membranes leads to issues both economically in the form of having to replace them but from an environmental standpoint it is unsustainable to continuously have to dispose of and manufacture replacement membranes. Cryogenic distillation offers a method of using nontoxic materials to produce high purity gas streams through the utilisation of low temperatures and high pressures which allows carbon dioxide to liquefy leaving a pure methane stream. However the energy cost associated with this method is massive which makes it less sustainable and exceedingly costly.[2]

It is for these reasons that we seek to create novel materials which will be more efficient, more sustainable and economically viable. Initial work will consist of the use of deep eutectic solvents in conjunction with other sorbents to increase their upgrading capabilities.

Work to date

**CO₂ uptake in TOPO-based hydrophobic low melting mixtures**

The screening methodology has improved since previous reports with the utilisation of our own recently repaired head-space gas chromatograph (HS-GC). This has increased the maximum screening pressure to around 3.5 bar, extending the scope from the upper limit of 1.8 bar as described in the previous report.

Hydrophobic low melting mixtures (HLMMs) have been a major focus of my research this quarter. They have been previously synthesised in QUILL based on trioctylphosphine oxide (TOPO) combined with acid hydrogen-bond donors (Fig 1) and have substantially lower viscosity than many other reported LMMs such as choline chloride based mixtures.[3]
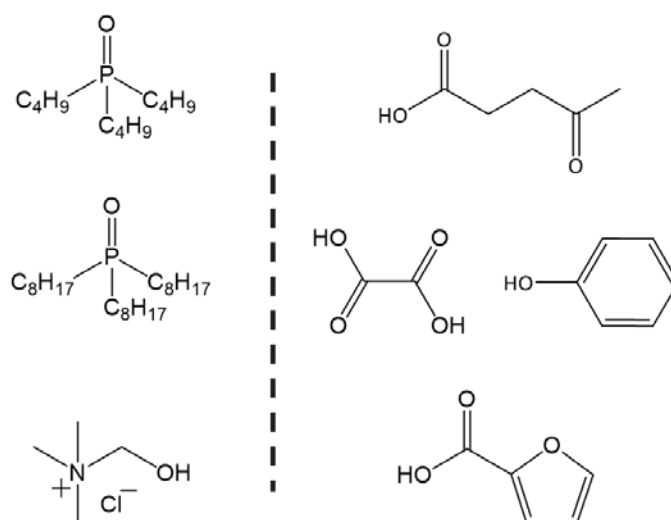

Figure 1 - Structures of hydrogen bond acceptor (left) and hydrogen bond donor (right) components of TOPO-based HLMMs used in this work

Gas uptake measurements have shown that these materials have exceptionally high CO_2 uptake when compared with other DES physisorbants such as choline chloride:urea ([Ch]Cl:U]) 1:2. Exceptional CO_2 uptakes are found in the TOPO:Lev 1:2 system where we see CO_2 capacities higher than that of one of the best ionic liquid [BMIM][NTf₂]. This has been attributed to the presence of the phosphine oxide group in the HLLM interaction strongly with CO_2 as has previously been seen in porous polymers but never before in LMMs.[4] There is also a likelihood that the levulinic acid plays an important role in the results but it's exact function has not yet been elucidated. Several other HBDs were tested but they did not show uptakes as high as that of levulinic acid or phenol.
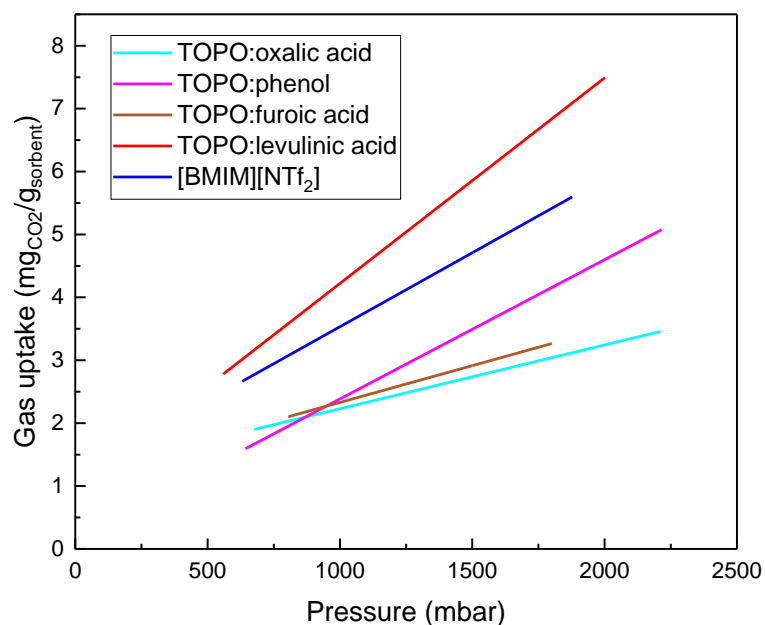
Figure. 2 - Plot of CO_2 uptake in mg/g as a function of pressure in various TOPO based deep eutectic solvents using [BMIM][NTf$_2$] as a comparative standard ionic liquid

The most promising material was then taken forward to be tested in a mixed gas scenario using a 50/50 CO_2/CH_4 (molar) gas mixture. Figure 3 shows that the TOPO:levulinic acid system along with high CO_2 capacity has high selectivity for CO_2 over CH_4 again comparable to that of [BMIM][NTf$_2$] although the slight increase in CH_4 capacity of our system must be noted. CO_2 capacities do not decrease when comparing partial pressure with that of pure gas. This could indicate that the modes of absorption of CO_2 and CH_4 are not competitive.
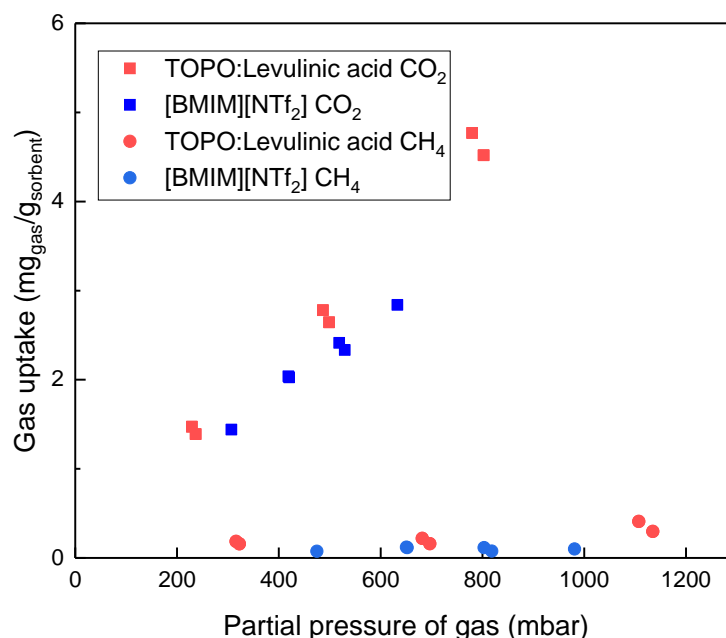
Figure 3 - Comparison of CO_2 and CH_4 uptakes from a 50/50 (molar) gas mixture using TOPO:Levulinic acid and [BMIM][NTf$_2$] as sorbents

Synthesis of deuterated randomly methylated beta cyclodextrin (RAMEB)

Most of my time this quarter has been devoted to synthesis of RAMEB several different strategies were attempted. Initially with direct deuteration utilising a Ru/C catalyst in D_2O. This was however found to lead to low degrees of methylation which were suitable for neutron scattering. This led to the second approach where we initially deuterated the natural beta cyclodextrin to 30% deuteration. This was then followed by partial methylation with iodomethane d$_3$. This method did not lead to a high enough methylation level so was followed with a much safer methylation step with in house synthesised dimethyl sulfate d$_6$. This resulted in a highly deuterated sample of RAMEB-d which will used for neutron scattering experiments.

Future work

Elucidation of the exact mechanism of absorption of the TOPO:levulinic acid system will be a focus in the near future as we could take this knowledge forward to improve the system further. Exchanging TOPO for other phosphine oxides could yield improved results also.

In regards to RAMEB neutron scattering experiments the synthesised RAMEB d will used at ISIS to gain structural information about supramolecular deep eutectic solvents.

References

1. F. M. Baena-Moreno, M. Rodríguez-Galán, F. Vega, L. F. Vilches and B. Navarrete, *Int. J. Green Energy*, 2019, **16**, 401–412.
2. M. R. Rodero, R. Ángeles, D. Marín, I. Díaz, A. Colzi, E. Posadas, R. Lebrero and R. Muñoz, in *Biogas*, Springer, 2018, pp. 239–276.
3. E. L. Byrne, R. O'Donnell, M. Gilmore, N. Artioli, J. D. Holbrey and M. Swadźba-Kwaśny,

Phys. Chem. Chem. Phys., 2020, **22**, 24744–24763.

4.   S. Qiao, W. Huang, Z. Du, X. Chen, F.-K. Shieh and R. Yang, *New J. Chem.*, 2015, **39**, 136–141.

5.   H. Kim, Y. Kim, M. Yoon, S. Lim, S. M. Park, G. Seo and K. Kim, *J. Am. Chem. Soc.*, 2010, **132**, 12200–12202.